Published in final edited form as:
Curr Drug Metab. 2011 October ; 12(8): 774–792.

PET and SPECT Radiotracers to Assess Function and Expression of ABC Transporters in Vivo

Severin Mairinger[1,2,3], **Thomas Erker**[3], **Markus Müller**[2], and **Oliver Langer**[1,2,*]

[1]Health and Environment Department, Molecular Medicine, AIT Austrian Institute of Technology GmbH, Seibersdorf, Austria

[2]Department of Clinical Pharmacology, Medical University of Vienna, Vienna, Austria

[3]Department of Medicinal Chemistry, University of Vienna, Vienna, Austria

Abstract

Adenosine triphosphate-binding cassette (ABC) transporters, such as P-glycoprotein (Pgp, ABCB1), breast cancer resistance protein (BCRP, ABCG2) and multidrug resistance-associated proteins (MRPs) are expressed in high concentrations at various physiological barriers (e.g. blood-brain barrier, blood-testis barrier, blood-tumor barrier), where they impede the tissue accumulation of various drugs by active efflux transport. Changes in ABC transporter expression and function are thought to be implicated in various diseases, such as cancer, epilepsy, Alzheimer's and Parkinson's disease. The availability of a non-invasive imaging method which allows for measuring ABC transporter function or expression in vivo would be of great clinical use in that it could facilitate the identification of those patients that would benefit from treatment with ABC transporter modulating drugs. To date three different kinds of imaging probes have been described to measure ABC transporters in vivo: i) radiolabelled transporter substrates ii) radiolabelled transporter inhibitors and iii) radiolabelled prodrugs which are enzymatically converted into transporter substrates in the organ of interest (e.g. brain). The design of new imaging probes to visualize efflux transporters is *inter alia* complicated by the overlapping substrate recognition pattern of different ABC transporter types. The present article will describe currently available ABC transporter radiotracers for positron emission tomography (PET) and single-photon emission computed tomography (SPECT) and critically discuss strengths and limitations of individual probes and their potential clinical applications.

Keywords

ABC transporter; blood-brain barrier; breast cancer resistance protein; multidrug resistance-associated protein; P-glycoprotein; positron emission tomography; single-photon emission computed tomography

INTRODUCTION

Most drugs exert their effects not within the blood compartment, but in defined target tissues, where drug binding sites (e.g. enzymes, transporter proteins, ion channels, receptor proteins) are located and into which drugs have to distribute from the central compartment [1]. In many cases, the assumption that drug molecules can diffuse freely across cell membranes and reach a complete and lasting equilibrium between blood and tissue does not

*Corresponding author: Oliver Langer, PhD, Health and Environment Department, Molecular Medicine, AIT Austrian Institute of Technology GmbH, 2444 Seibersdorf, Austria, Tel.: +43 50 550 3496. Fax: +43 50 550 3473. oliver.langer@ait.ac.at.

Europe PMC Funders Author Manuscripts

hold true [2]. A major factor governing drug disposition in the body is the transport of drug molecules into and out of different body compartments by active transport proteins, such as those belonging to the adenosine triphosphate (ATP)-binding cassette superfamily [3-6]. The ABC transporters are encoded by 48 genes in the human genome and have been classified into seven subfamilies (ABCA-ABCG) based on their amino acid homology and domain organization. By using ATP-hydrolysis as energy source ABC transporters are able to transport a huge variety of structurally diverse molecules across membranes irrespective of concentration gradient. ABC transporters are ubiquitously expressed in the body, but show particularly high concentrations in excreting organs (liver, kidney) and physiological barriers, such as the blood-brain, -testis and -placenta barrier, where they protect the respective organs against the accumulation of toxins. Changes in ABC transporter function and expression are implicated in many different diseases. The most well known example is the multidrug resistant phenotype of tumors, which is characterized by the expression of high levels of P-glycoprotein (Pgp, ABCB1) and related transporters in the tumoral cell membrane [3, 6]. Another example is therapy refractory epilepsy which has been linked to a regional overexpression of Pgp and multidrug resistance-associated proteins (MRPs) in the blood-brain barrier (BBB) surrounding epileptic brain regions, where they impede access of antiepileptic drugs to their target structures in the central nervous system (CNS) by active efflux transport [4-5]. As opposed to cancer and epilepsy, decreased function of Pgp at the BBB has been suggested to occur in Parkinson's and Alzheimer's disease. In Parkinson's disease this is believed to lead to increased accumulation of environmental neurotoxins in the brain, which might contribute to neurodegenerative pathology [7]. In Alzheimer's disease impaired cerebral Pgp function might facilitate entry of beta-amyloid from blood into brain, thereby increasing the beta-amyloid plaque load in the brain [8-9].

An appealing strategy to overcome transporter-mediated drug resistance could be the concomitant use of drugs which inhibit transporter function and thereby improve accessibility of diverse drugs to the tissues targeted for treatment [6]. In order to better understand disease related alterations of ABC transporters the availability of a diagnostic method which allows for quantifying transporter function and expression in animal disease models and humans would be of considerable interest. The non-invasive nuclear imaging methods positron emission tomography (PET) and single-photon emission computed tomography (SPECT) allow for assessing the density or function of molecular targets in vivo by externally monitoring the tissue distribution of intravenously administered target-selective radiotracers [10-12]. These non-invasive imaging methods hold great promise in personalized medicine as they allow for identifying individual patients prior to treatment initiation, which (over)express a certain molecular target of interest [13-14]. PET and SPECT tracers for ABC transporters could be useful to preselect cancer patients [15] or epilepsy patients [16-17] with increased ABC transporter activity who will benefit from treatment with ABC transporter modulating drugs.

The development of new radiotracers for PET and SPECT imaging is a challenging task, which is affected by a low success rate, similar to the development of therapeutic drugs [18]. Effective radiotracers to visualize molecular targets need to fulfill certain key criteria, such as high affinity and selectivity for the molecular target of interest, a low degree of non-specific binding in tissue where molecular target is located and absence of radiolabelled metabolites which are taken up into tissue [18-20]. ABC transporters are a relatively new target in molecular imaging and only few review articles on this topic have appeared in the literature so far (see for example: [21-26]). The aim of this review article is to give an up to date overview of currently available PET and SPECT tracers to visualize ABC transporter function and expression and to critically discuss their individual strengths and shortcomings and possible applications in medical research.

OVERVIEW OF ABC TRANSPORTERS

P-glycoprotein

The most extensively studied ABC transporter to date is Pgp. It was first identified by Juliano and Ling in Chinese hamster ovary cells [27]. It is not only the first ABC transporter that was shown to be involved in the development of multidrug resistance of cancer cells, but also the first ABC transporter which was found in endothelial cells of the human BBB. Pgp is normally expressed in the transport epithelium of the liver, kidney and gastrointestinal tract, at pharmacological barrier sites, in adult stem cells and in assorted cells of the immune system. An exciting property of Pgp is the fact that it has very broad substrate specificity and is capable of transporting many therapeutic drugs. Pgp generally transports neutral and cationic hydrophobic compounds [28]. Further research showed that Pgp also exists in mammalian brain capillary endothelial cells, such as in primates, rats, mice, cattle and pigs. Due to this broad variety of findings, it was suggested that Pgp fulfills a key role as a defense mechanism at the mammalian BBB [5]. *Mdr1* knockout mice were shown to have an in some cases drastically increased brain exposure to Pgp substrates compared to wild-type mice [29]. Also treatment of animals with Pgp modulators such as cyclosporine A (CsA), valspodar (PSC833), zosuquidar (LY335979), elacridar (GF120988) or tariquidar (XR9576) was shown to result in increased concentration of Pgp substrate drugs, such as antiviral and anticancer drugs, in the CNS [5]. In the human body two different types of Pgp are expressed: type I encoded by *MDR1* (also known as *ABCB1)* and type II encoded by *MDR2*. Type I is expressed in the luminal membrane of cerebral endothelial cells and type II is present in the canalicular membrane of hepatocytes and functioning as phosphatidylcholine translocase [5]. Pgp type I consists of 1280 amino acids and its molecular weight is about 140-170 kDa depending on its glycolysation grade. In the human genome it is located on chromosome 7 and has 28 exons. The *N*-terminal half of the molecule contains 6 transmembrane domains (TMDs) followed by a large cytoplasmic domain with an ATP-binding site. Then a second section with 6 TMDs followed by another ATP-binding site, which shows over 65% of amino acid similarity with the first half of the polypeptide, is present. The TMDs are interacting with the substrate and are responsible for its recognition. With the alteration of the binding or changes of the conformation triggered by a single mutation in any transmembrane region the whole transport would be changed [30]. In contrast, the non-binding domains (NBDs) are not involved in the substrate recognition, but they are crucial for the transport mechanism. If a substrate is present the NBDs change their position relatively to the cell membrane. For this conformational change energy must be provided.

In rodents, the multidrug resistance type I Pgp is encoded by two genes (*Mdr1a or Abcb1a* and *Mdr1b* or *Abcb1b*). The substrate specificity of *Mdr1a* and *Mdr1b* Pgp in rodents is different but partly overlapping, and together the two rodent genes are expressed in roughly the same manner as the single human *MDR1* gene, suggesting that they perform the same set of functions in rodents as the *MDR1* Pgp in humans [5].

Breast cancer resistance protein (BCRP)

Breast cancer resistance protein (BCRP, ABCG2) belongs to the ABCG subfamily, and has first been described by Doyle *et al.* in a drug resistant MCF-7 breast cancer subline [31]. The murine homologue of human BCRP is called Bcrp1 (Abcg2). In contrast to Pgp and MRP1, BCRP is considered as half-transporter, similar to all other members of the ABCG subfamily. The expression pattern of BCRP in normal tissues is consistent with a role in protection against xenobiotics with significant levels in the small intestine, colon, liver, CNS, capillary endothelium, testis, ovary and placental syncytiotrophoblasts [32-33]. Considering BCRPs localization at the luminal surface of the microvessel endothelium in

the brain, it most likely also contributes to the BBB together with Pgp and MRPs. Interestingly, whereas expression of Pgp is higher than that of Bcrp1 in the murine BBB [34], the opposite seems to be true in humans. Recent data show that mRNA levels of BCRP are about eightfold higher than Pgp mRNA levels in human brain capillaries [35]. In another study, BCRP expression levels in cynomolgus monkey brain microvessels were quantified with liquid-chromatography mass spectrometry/mass spectrometry (LC-MS/MS) and found to be 3.5-fold higher than in mouse brain whereas Pgp expression levels were 0.3 fold lower [36]. However, as BCRP has a substantial overlap in substrate specificity with Pgp [37], the functional role of BCRP at the BBB has remained elusive, despite the availability of Bcrp1-deficient mice [29]. BCRP is also highly expressed on the surface of hematopoetic and most likely other stem cells, consistent with a protective role. BCRP has also been implicated as a contributing transporter to multidrug resistance in cancer, although clinical findings remain somewhat controversial [33]. In general BCRP transports large hydrophobic molecules which can be either positively or negatively charged. BCRP transports various chemotherapeutic agents, such as mitoxantrone, flavopiridol, methothrexate, as well as molecules pertaining to other pharmacological classes [33]. Importantly there are significant overlaps between substrates of BCRP, MRP1 and Pgp. Since the discovery of BCRP in 1996 up to now only a few selective BCRP inhibitors have been reported. Fumitremorgin C, a diketopiperazine, isolated from *Aspergillus fumigatus*, was reported first [38], but cannot be used in vivo due to its neurotoxicity. Ko143 [39], a structural analogue of fumitremorgin C, has been reported to inhibit BCRP with higher potency than fumitremorgin C [40] and can also be used in vivo [41]. However, whereas Ko143 seems to be selective for BCRP over Pgp and MRP1 [39], some cross reactivity with MRP2 has been reported [37, 40].

Multidrug resistance-associated proteins (MRPs)

The family of multidrug resistance-associated proteins or ABCC family has currently 19 members, nine of which are found in humans (ABCC1-ABCC9). One important representative is MRP1 (ABCC1), which is a 190 kDa protein consisting of 1531 amino acids. In comparison to Pgp, MRP1 possesses an additional TMD composed of 5 α-helical segments. MRP1 was discovered in 1992 in a multidrug resistant human small cell lung cancer cell line [42]. MRP1 is ubiquitously expressed in normal tissue and can also be found at the BBB and blood-cerebrospinal fluid (CSF) barrier [43]. It is the main active transporter of molecule conjugates to glutathione, glucuronide or sulfate and unconjugated compounds, taking the role of an organic ion transporter. The role of MRP1 as an efflux transporter at the BBB remains controversial. An in vivo study showed that following intracerebral microinjection of the endogenous metabolite 17beta-estradiol-D-17beta-glucuronide, the extrusion rate from the brain was significantly retarded in *Abcc1*$^{-/-}$ mice as compared to wild-type mice [44]. However, other in vivo studies using the in situ brain perfusion technique have shown that MRP1 has no functional effect at the BBB [45-46]. Comparisons of *Abcb1a*$^{-/-}$*/Abcb1b*$^{-/-}$*/Abcc1*$^{-/-}$ *and Abcb1a*$^{-/-}$*/Abcb1b*$^{-/-}$ mice revealed that mice deficient for both Pgp and Mrp1 have approximately 10-fold higher etoposide concentrations in the CSF than mice that lack Pgp but express Mrp1, indicating that Mrp1 critically contributes to the permeability of the blood–CSF barrier [47]. MRP2 and MRP4 are located on the apical side of cell membranes where they efflux cytotoxic compounds just as Pgp and BCRP does, whereas MRP1, MRP3 and MRP5 are found to be located basolaterally in most cell types [5]. MRP2 is expressed at canalicular membranes of hepatocytes, transporting several conjugated compounds into bile. MRPs located at the apical side of the blood capillary endothelial cells restrict brain access of MRP substrates by efflux transport.

MRPs can be inhibited in vitro and in vivo by using MRP inhibitors, such as probenecid or MK-571 [5]. For instance brain uptake of fluorescein in mice [48-49] and of phenytoin in

rats [50] has been shown to be increased after probenecid administration. However, probenecid is not an MRP selective inhibitor as it also inhibits organic anion transporting polypeptides (OATP) and organic anion transporters (OATs). MK-571 has recently been shown to inhibit Pgp and BCRP with comparable potencies as MRP2 [37].

POSITRON EMISSION TOMOGRAPHY AND SINGLE PHOTON EMISSION COMPUTED TOMOGRAPHY

PET and SPECT are powerful non-invasive nuclear medicine imaging techniques providing good spatial resolution and high sensitivity [10-12]. For PET and SPECT imaging radiolabelled molecules, so called radiotracers, are usually administered by intravenous injection. PET or SPECT cameras monitor the distribution of these radiotracers in the living organism over time. The concentration-time curves of radiotracers are analyzed by biomathematical modelling to derive measures of in vivo neurochemistry (e.g. blood flow, glucose metabolism rate, density of receptor proteins) [51]. The great advantage of PET over SPECT is a higher sensitivity, better temporal and spatial resolution and the ability to provide a quantitative measure of radioactivity in tissue. These methods are particularly attractive to clinical researchers, because they can be applied to the living human brain. PET typically makes use of the radioisotopes carbon-11 (^{11}C), nitrogen-13 (^{13}N), oxygen-15 (^{15}O), fluorine-18 (^{18}F) or gallium-68 (^{68}Ga). These decay by emitting a positron, with radioactive half-lives of 20.4, 9.96, 2.04, 109.7 and 67.6 min, respectively. The emitted positron annihilates with an electron and emits two co-linear annihilation photons (gamma rays) that can be detected outside the body. Typically, the radioisotopes are generated in a cyclotron and because of their short half-lives need to be rapidly incorporated into the molecule of interest immediately prior to administration. In SPECT, isotopes that decay by electron capture and/or γ emission are used, and include both iodine-123 (^{123}I, half-life: 13.1 h) and technetium-99m (^{99m}Tc, half-life: 6.01 h).

RADIOLIGANDS FOR ABC TRANSPORTERS

The design of radiotracers to visualize ABC transporters is not a trivial task. As their name implies multidrug transporters are made to transport a multitude of different chemical compounds. Individual transporters, such as Pgp and BCRP, show considerable overlap in substrate recognition patterns. The probably most critical issue in the development of ABC transporter ligands is therefore to achieve selectivity among different transporter types. Another critical issue, which holds particularly true for imaging of cerebral Pgp and BCRP, is the fact that almost all ligands known to date are highly lipophilic molecules, with log *P* values >3, which is usually considered the cut-off for successful CNS radioligands [18]. Almost all efforts to develop ABC transporter ligands have so far concentrated on Pgp expressed at the BBB or in tumors. To date three different kinds of imaging probes have been described to measure ABC transporters in vivo: i) radiolabelled transporter substrates ii) radiolabelled transporter inhibitors and iii) radiolabelled prodrugs which are enzymatically converted into transporter substrates in the organ of interest (e.g. brain). The first class of compounds is the most extensively studied one and has produced effective imaging probes such as (*R*)-[^{11}C]verapamil or [^{11}C]-*N*-desmethyl-loperamide which have already been used to study transporter function in vivo in humans. However, whereas these radiotracers are excellent tools to study pharmacological Pgp modulation they are not well suited to study differences of transporter function in different brain regions due to their low brain uptake (standardized uptake value, SUV<1). In order to overcome the limitations of substrate probes several third-generation Pgp inhibitors, such as [^{11}C]laniquidar, [^{11}C]elacridar and [^{11}C]tariquidar, were developed. The initial idea behind the development of radiolabelled Pgp inhibitors was to come up with radiotracers that should bind to Pgp without being transported by it and therefore afford radiotracer with higher baseline PET

signals than substrates and which should allow for mapping of Pgp expression levels. Unfortunately, all Pgp inhibitors developed to date have not come up to these expectations and were shown to behave in vivo very similar to radiolabelled substrates. The last approach to visualize ABC transporters has so far been only applied to imaging of cerebral MRP1 [26]. Herein, a radiolabelled prodrug is administered which lacks affinity to efflux transporters. Inside the brain the prodrug is metabolically converted into a substrate drug, the efflux of which serves as a direct indicator of MRP1 activity. The concept is very appealing in that it elegantly solves the problem of low brain PET signals obtained with ABC transporter substrate radiotracers. It remains to be seen however if this method of signal amplification can be applied to other ABC transporter families, such as Pgp. In the following we will review radiotracers which have been developed so far to visualize ABC transporters.

RADIOLABELLED PGP SUBSTRATES

Rac-[^{11}C]verapamil and (*R*)-[^{11}C]verapamil

The calcium channel inhibitor verapamil is used as a reference Pgp inhibitor in experimental pharmacology [5]. At tracer concentrations as used in PET experiments, verapamil is transported by Pgp and ^{11}C-labelled verapamil has therefore been developed at the University Medical Center Groningen (The Netherlands) as the first Pgp substrate radiotracer [52]. However, there is some evidence that verapamil is also a substrate of MRP1 [53], although this has so far not been proven at tracer levels. [^{11}C]Verapamil has been used either as the racemate or as the *(R)*-enantiomer. Elsinga *et al.* first synthesized *rac*-[^{11}C]verapamil in 1996 by reacting *N*-desmethyl-verapamil with [^{11}C]CH_3I [54]. *Rac*-[^{11}C]verapamil has been evaluated in vitro by using human ovarian cell lines and their adriamycin resistant counterpart. The intracellular concentration of *rac*-[^{11}C]verapamil was 4-5 times higher in the sensitive compared to the resistant cell line with high Pgp expression. Biodistribution studies with *rac*-[^{11}C]verapamil demonstrated 9.5-fold and 3.4-fold higher activity concentrations in brain and testes of *Abcb1a*$^{-/-}$ as compared to wild-type mice, respectively [52]. Administration of 50 mg/kg CsA increased brain and testes uptake of activity in wild-type mice, by 10.6-fold and 4.1-fold, respectively, whereas *Abcb1a*$^{-/-}$ mice showed no effect on CsA treatment. Studies in rats bearing tumors bilaterally, a Pgp negative small cell lung carcinoma (GLC_4) and its Pgp overexpressing subline (GLC_4/Pgp) showed 185% higher *rac*-[^{11}C]verapamil activity levels in GLC_4 compared to GLC_4/Pgp tumors. Administration of CsA (50 mg/kg) raised the activity concentration in GLC_4/Pgp tumors (+184%) to the level of non Pgp overexpressing tumors. Additionally, a 1280% increase in brain activity was observed after CsA administration [55]. In another study it was shown in rats that the volume of distribution (V_T) of *rac*-[^{11}C]verapamil in brain can be used as a quantitative parameter of Pgp function at the BBB, as V_T was shown to increase dose-dependently following administration of different CsA doses [56]. Syvänen and co-workers presented a new and very elegant approach to study CsA-induced inhibition of cerebral Pgp by administering *rac*-[^{11}C]verapamil as a constant infusion and by giving the inhibitor as an intravenous (i.v.) bolus when steady-state concentrations of *rac*-[^{11}C]verapamil in plasma and brain were achieved [57]. A similar approach was later used in studies with (*R*)-[^{11}C]verapamil, in which unlabelled inhibitor (tariquidar) was given during rather than before the (*R*)-[^{11}C]verapamil PET scan, at a time point when activity had reached pseudo steady state in plasma and brain [58-59]. The synthesis of *rac*-[^{11}C]verapamil was improved in terms of radiochemical yield by using [^{11}C]methyl triflate instead of [^{11}C]CH_3I as the methylating agent [60]. The first human evaluation of *rac*-[^{11}C]verapamil was conducted in five cancer patients, where 43.0±5.3, 1.3±0.2 and 0.9±0.3% of the injected dose (ID) were found in lungs, heart and tumor, respectively [61]. In another human study healthy volunteers underwent paired PET scans with *rac*-[^{11}C]verapamil before and during infusion of CsA, at a dose which was several-fold higher than usually given in the clinic (2.5 mg/kg/1

h for 2 h) [62]. Despite the fact that arterial blood sampling was also performed, brain activity uptake was only quantified in terms of ratio of the area under the concentration-time curve (AUC) in brain to that in blood (AUC_{brain}/AUC_{blood}), which was found to be increased by 88±20% during CsA treatment. This important study provided the first proof in humans that *rac*-[^{11}C]verapamil is transported by Pgp at the BBB by employing CsA as a blocking agent of Pgp. The data from this paper were later on re-analyzed in another study by kinetic modelling which showed that a 2-tissue-4-rate-constant (2T4K) model best described *rac*-[^{11}C]verapamil brain kinetics after Pgp inhibition [63]. The influx rate constant K_1 and V_T were found to be increased by 73% and 67% after CsA administration, respectively. The increase of K_1 caused by Pgp inhibition is in line with the concept that Pgp acts as a gatekeeper at the BBB and prevents substrates from diffusing across the luminal endothelial cell membrane. In addition it was reported that Pgp function can be effectively measured using only the first 10 min of the PET data (where metabolism of *rac*-[^{11}C]verapamil is low) and a 1-tissue-2-rate-constant (1T2K) model. Similar findings have been also made in an earlier publication by a Japanese group which employed a graphical analysis method of the PET data acquired during the initial few minutes after radiotracer injection [64]. In a non-human primate study a similar set-up was used as in the Sasongko study employing another inhibitor of Pgp, namely valspodar (PSC833), which was given as an i.v. infusion at a dose of 20 mg/kg/2h and led to a 2.3-fold increase in the AUC_{brain}/AUC_{blood} ratio compared to baseline scans [65]. In another study, pregnant non-human primates underwent *rac*-[^{11}C]verapamil PET scans before and after CsA administration (12 or 24 mg/kg/h) to measure placental Pgp activity either in mid- or late-gestational age [66-67]. Percent change in $AUC_{fetal\ liver}/AUC_{maternal\ plasma}$ ratio after CsA administration was used as a surrogate marker of placental Pgp activity and was found to significantly increase from mid-(+35±25%) to late gestation (+125±66%), which the authors interpreted as increasing Pgp activity with gestational age [66]. Two studies have assessed the effect of functional single nucleotide polymorphisms in the *ABCB1* gene in healthy volunteers on brain penetration of *rac*-[^{11}C]verapamil and failed to show differences in *rac*-[^{11}C]verapamil brain kinetics between different *ABCB1* haplotypes [68-69].

As for quantitative PET studies an enantiomerically pure PET tracer is preferred over a racemic mixture, the synthesis of the individual enantiomers of [^{11}C]verapamil was developed [70]. Biodistribution studies in wild-type and *Abcb1a*$^{-/-}$/*Abcb1b*$^{-/-}$ mice showed similar organ uptake values for both [^{11}C]verapamil enantiomers with 14.7 and 18.7 times higher activity uptake in brains of *Abcb1a*$^{-/-}$/*Abcb1b*$^{-/-}$ as compared to wild-type mice for (*R*)- and (*S*)-[^{11}C]verapamil, respectively [71]. As the in vitro efflux ratios of (*R*)- and (*S*)-verapamil were also similar in LLC-PK1 MDR cells it was concluded that both enantiomers showed similar Pgp substrate properties. As (*R*)-verapamil is less metabolized than the (*S*)-enantiomer in humans [72] and has lower affinity for calcium channels, (*R*)-[^{11}C]verapamil was proposed as the preferred candidate for PET imaging. Metabolism of (*R*)-[^{11}C]verapamil was analyzed in Wistar rats by employing a combined solid-phase extraction (SPE) high-performance liquid chromatography (HPLC) protocol [73]. At 60 min after (*R*)-[^{11}C]verapamil injection 28.1±2.7% of total activity in plasma and 47.7±10.5% in brain were in the form of unchanged parent. The remainder of activity was mainly composed of polar [^{11}C]metabolites, putatively the *N*-demethylation product [^{11}C]formaldehyde and related species. The significant brain uptake of polar [^{11}C]metabolites seen in rats can be considered as problematic as it presumably occurs independently of Pgp function. Test-retest (*R*)-[^{11}C]verapamil PET scans and arterial blood sampling were performed in healthy human volunteers to develop a kinetic model for quantification of Pgp function at the BBB [74]. As (*R*)-[^{11}C]verapamil gives radiolabelled metabolites in humans which are also Pgp substrates (the *N*-dealkylation products [^{11}C]D617 and [^{11}C]D717) [75] these metabolites were lumped together with unchanged (*R*)-[^{11}C]verapamil in the arterial input function assuming that their in vivo behavior was similar to that of (*R*)-[^{11}C]verapamil [74].

Therefore an one input, one-tissue compartment model with correction for *N*-demethylated metabolites only was proposed as the model of choice which provided good compromise between fit quality and test-retest variability [74]. Unfortunately, later studies in which rats were scanned with [^{11}C]D617 before and after tariquidar administration (15 mg/kg) suggested that [^{11}C]D617 may in fact be a weaker Pgp substrate than (*R*)-[^{11}C]verapamil itself, which questions the validity of the initially proposed model.[1] The already complex situation for the kinetic modelling of (*R*)-[^{11}C]verapamil was further complicated by the observation that in medically refractory epilepsy patients the fraction of polar [^{11}C]metabolites of (*R*)-[^{11}C]verapamil in plasma was up to two fold greater than in healthy control subjects, which was attributed to hepatic cytochrome P450 enzyme induction by antiepileptic treatment [76]. Luurtsema has shown in an earlier study that the polar [^{11}C]metabolite fraction of (*R*)-[^{11}C]verapamil is taken up into brain in rats [73]. If this holds true for humans as well, differences in peripheral (*R*)-[^{11}C]verapamil metabolism between different study groups might compromise the quantitative measurement of Pgp function.

As brain uptake of (*R*)-[^{11}C]verapamil is quite low in baseline scans (SUV<1), which does not allow for measurement of regional differences in cerebral Pgp function, a double-scan paradigm consisting of (*R*)-[^{11}C]verapamil PET scans before and after administration of the potent, non-toxic Pgp/BCRP inhibitor tariquidar was proposed [77]. The great advantage of using tariquidar instead of CsA as an inhibitor is that tariquidar is safer, less toxic and more selective for Pgp than CsA [15]. It was shown that in rats i.v. administration of tariquidar at a dose of 15 mg/kg led to an 12-fold increase in whole-brain V_T of (*R*)-[^{11}C]verapamil [77]. In a follow-up study a detailed dose-response assessment of tariquidar and the structurally related Pgp/BCRP inhibitor elacridar was performed in rats giving half-maximum effect dose (ED_{50}) estimates of 3.0±0.2 and 1.2±0.1 mg/kg for tariquidar and elacridar, respectively, for increasing (*R*)-[^{11}C]verapamil whole-brain V_T [58]. It was suggested that performing (*R*)-[^{11}C]verapamil PET scans after half-maximum Pgp inhibition might be better suited to study regional differences in cerebral Pgp function than baseline scans alone [58]. A proof-of-concept study was performed in rats at 48 h after pilocarpine-induced status epilepticus (SE), a model of regional cerebral Pgp overexpression [78]. Both control and 48 h post-SE rats underwent (*R*)-[^{11}C]verapamil PET scans after administration of tariquidar at the ED_{50} (3 mg/kg).[2] PET data were region wise modelled using a 2T4K model and Pgp expression was independently quantified in the same brain regions using immunohistochemical staining.[2] In brain regions with increased Pgp expression (cerebellum, thalamus, hippocampus), V_T and K_1 of (*R*)-[^{11}C]verapamil were significantly decreased and k_2 increased relative to control animals, giving strong support that the employed PET imaging approach was indeed able to quantify regional cerebral Pgp function in this animal model.[2] In a similar study, no differences in (*R*)-[^{11}C]verapamil brain kinetics were found between control rats and rats at 7 days after kainate-induced SE before and after tariquidar administration (15 mg/kg), which was consistent with absence of differences in cerebral Pgp expression levels between the two groups found by immunohistochemical staining [79]. A possible methodological limitation of this study is that the employed tariquidar dose (15 mg/kg) resulted in maximal blockade of cerebral Pgp making (*R*)-[^{11}C]verapamil brain kinetics independent of Pgp function.

[1]Verbeek, J.; Syvänen, S.; Luurtsema, G.; de Lange, E. C.; Eriksson, J.; Windhorst, A. D.; Lammertsma, A. A., Initial PET studies in rats with novel radiotracer [^{11}C]D617 and comparison with (R)-[^{11}C]verapamil [symposium abstract]. *Neuroimage*, **2010**, *52* (Supplement 1), S26.

[2]Bankstahl, J. P.; Kuntner, C.; Bankstahl, M.; Wanek, T.; Stanek, J.; Müller, M.; Langer, O.; Löscher, W., An improved method to measure cerebral P-glycoprotein function reveals changes in brain uptake of (*R*)-[^{11}C]-verapamil following status epilepticus in rats [symposium abstract]. *J. Cereb. Blood Flow Metab.*, **2009**, *29* (S1), 222.

The promising concept of performing (*R*)-[^{11}C]verapamil PET scans after sub-maximal blockade of cerebral Pgp was translated to healthy human subjects, who were scanned with (*R*)-[^{11}C]verapamil before and after i.v. infusion of tariquidar at a dose of 2 mg/kg [59]. The data were analyzed by a 2T4K model which showed increases in whole-brain V_T and K_1 of +24±15% and +49±36%, respectively, after tariquidar administration. Importantly, it was shown that tariquidar administration had no effect on *(R)*-[^{11}C]verapamil metabolism and plasma protein binding. The data from this first human PET study employing tariquidar were re-analyzed region wise using an automated atlas approach to define 43 different brain regions of interest as well as statistical parametrical mapping (SPM) analysis [80]. No regional differences in tariquidar-induced Pgp inhibition were detected, which suggested that there were no pronounced regional differences in Pgp function in the healthy human brain [80]. These findings were shortly afterwards confirmed in a similar study employing *rac*-[^{11}C]verapamil and CsA as the inhibitor [81]. Higher doses than the 2 mg/kg dose of tariquidar (up to 8 mg/kg) have already been given to healthy human subjects without occurrence of severe adverse effects [82].[3] Bauer *et al.* reported an ED_{50} of 3.09±0.30 mg/kg for tariquidar to increase (*R*)-[^{11}C]verapamil whole-brain V_T in humans [3], which was remarkably similar to the value previously determined in rats (3.0±0.2 mg/kg) [58]. However, the maximum increase in (*R*)-[^{11}C]verapamil brain V_T relative to baseline scans was several-fold lower in humans (2.4 fold) as compared to rats (10.7-fold).[3] Three independent PET studies with either *rac*-[^{11}C]verapamil [83] or (*R*)-[^{11}C]verapamil [84-85] in small cohorts of young and aged healthy subjects showed that brain V_T increased as a function of age suggesting that Pgp activity at the BBB might decrease with age. First pilot data with (*R*)-[^{11}C]verapamil in Alzheimer patients suggest an about 2-fold increased cerebral binding potential (BP_{ND}) of (*R*)-[^{11}C]verapamil, which was estimated using a constrained two-tissue compartment model, relative to age-matched control subjects.[4]

A pilot PET study with (*R*)-[^{11}C]verapamil was conducted in seven patients with medically refractory temporal lobe epilepsy [86]. A 1T2K model was used to estimate K_1, k_2 and V_T values in different temporal lobe brain regions of interest (ROIs) which were compared between the hemisphere located ipsilaterally and contralaterally to the seizure focus. Although some brain regions in some patients were shown to have ipsilaterally decreased V_T and increased k_2 values, which was consistent with ipsilaterally increased Pgp efflux, the high variability of the data combined with the small sample size failed to reveal any statistically significant differences in regional Pgp function in this patient group [86]. Importantly, it was shown that high radioactivity uptake in the plexus choroideus contaminated the PET signal in the adjacent hippocampus precluding the analysis of this region, at least when employing a low-resolution PET camera as the GE Advance scanner [86]. A better suited approach to delineate regional differences in Pgp function in the brains of therapy refractory epilepsy patients might be the performance of paired *(R)*-[^{11}C]verapamil scans before and after administration of tariquidar, which has already been presented in abstract form.[5] A series of studies with *rac*-[^{11}C]verapamil investigated regional brain V_Ts employing SPM analysis in different disease conditions (Parkinson's disease, depression, schizophrenia) [87-90]. Although certain regional differences were detected in patient groups compared to control subjects there is concern that at least part of

[3]Bauer, M.; Zeitlinger, M.; Matzneller, P.; Stanek, J.; Lackner, E.; Wadsak, W.; Müller, M.; Langer, O., Dose-response assessment of tariquidar for inhibition of P-glycoprotein at the human blood-brain barrier using (*R*)-[^{11}C]verapamil PET [symposium abstract]. *BMC Pharmacol.*, **2010**, *10* (Supplement 1), A47.

[4]van Assema, D. M. E.; Lubberink, M.; Hoetjes, N. J.; Hendrikse, H.; Schuit, R. C.; Windhorst, A. D.; van der Flier, W. M.; Philip Scheltens, P.; Lammertsma, A. A.; van Berckel, B. N. M., Decreased Pglycoprotein function at the blood-brain barrier in patients with Alzheimer's disease as shown by (*R*)-[^{11}C]verapamil and PET [symposium abstract]. *Neuroimage*, **2010**, *52* (Supplement 1), S53.

[5]Feldmann, M.; Asselin, M. C.; Wang, S.; McMahon, A.; Walker, M.; Jose Anton, J.; Hinz, R.; Sisodiya, S.; Duncan, J.; Koepp, M., Tariquidar inhibition of P-glycoprotein activity in patients with temporal lobe epilepsy measured with PET and (*R*)-[C-11]Verapamil [symposium abstract]. *Neuroimage*, **2010**, *52* (Supplement 1), S148.

these differences might have been driven by morphological brain changes leading to different degrees of spill-in of radioactivity from the ventricle system, rather than by differences in Pgp function.

[^{11}C]Loperamide and [^{11}C]-*N*-desmethyl-loperamide

Loperamide is an opiate receptor agonist which does not have CNS side effects, which can be attributed to the molecule being an avid substrate of Pgp at the BBB. [^{11}C]Loperamide was first synthesized by researchers at GlaxoSmithKline by methylation of *N*-desmethyl loperamide with [^{11}C]CH_3I.[6] A first in vivo evaluation in Yorkshire landrace pigs showed very low brain activity uptake in baseline scans (<0.001% ID/ml), which was dose-dependently increased after administration of different CsA doses (1-30 mg/kg) with a maximum increase of 7-fold compared to baseline scans.[6] In a clinical PET study, which was only published in abstract form,[7] three healthy volunteers were scanned with [^{11}C]loperamide under baseline conditions or after i.v. administration of CsA (10 mg/kg, i.v.) which lead to a 2-fold increased brain activity influx rate constant K_1 compared to baseline scans. After these initial investigations with [^{11}C]loperamide at GlaxoSmithKline, the PET group at the National Institute of Health (USA) started to work with this radiotracer. These researchers conducted studies with [^{11}C]loperamide in wild-type and *Abcb1a*$^{-/-}$ /*Abcb1b*$^{-/-}$ mice as well as in non-human primates [91]. Baseline scans in monkeys showed low brain activity uptake (0.4 SUV); pretreatment of the animals with tariquidar or a novel third-generation Pgp inhibitor named DCPQ, which is structurally related to zosuquidar, led to increased activity levels in brain with maximal effects (3.5 fold increases relative to baseline) at inhibitor doses of 8 mg/kg. Radio-HPLC analysis showed 16-fold higher concentrations levels of [^{11}C]loperamide in *Abcb1a*$^{-/-}$ /*Abcb1b*$^{-/-}$ than in wild-type mouse brain. In addition, one radiolabelled metabolite of [^{11}C]loperamide, which was identified as [^{11}C]-*N*-desmethyl loperamide, was shown to account for 24% of total brain activity in *Abcb1a*$^{-/-}$ /*Abcb1b*$^{-/-}$ mice and to have 17-times higher brain concentrations in *Abcb1a*$^{-/-}$ /*Abcb1b*$^{-/-}$ than in wild-type animals [91]. The authors suggested [^{11}C]-*N*-desmethyl loperamide as a superior PET tracer to [^{11}C]loperamide as it was expected to generate one radiometabolite less than [^{11}C]loperamide and as it had been shown to be an avid Pgp substrate.

Experiments with tritium-labelled *N*-desmethyl loperamide in human cell lines overexpressing either Pgp or BCRP or MRP1 revealed that *N*-desmethyl loperamide was selectively transported by Pgp [92]. [^{11}C]-*N*-desmethyl loperamide was synthesized from its *N*-desmethyl precursor by methylation with [^{11}C]CH_3 I [93]. Consistent with the previous results obtained with [^{11}C]loperamide, [^{11}C]-*N*-desmethyl loperamide showed negligible brain activity uptake in wild-type mice, non-human primates and humans, which could be dose-dependently increased by preadministration of either DCPQ (non-human primates) or tariquidar (humans) [82, 93-94]. Maximum increases compared to baseline scans were 7-fold in monkeys after 8 mg/kg DCPQ [94] and 4-fold in humans after 6 mg/kg tariquidar [82]. Brain washout of [^{11}C]-*N*-desmethyl loperamide was very slow under conditions of Pgp blockade, which was explained by trapping of this radiotracer in lysosomes in brain tissue [95]. Administration of the opiate receptor antagonist naloxone during [^{11}C]-*N*-desmethyl loperamide PET scans in monkeys exerted no effect on brain time-activity curves indicating that the PET signal of [^{11}C]-*N*-desmethyl loperamide was not influenced by opiate receptor binding [94]. Importantly, Liow *et al.* showed that brain activity uptake of

[6]Passchier, J.; Lawrie, K.; Bender, D.; Fellows, I.; Gee, A., [^{11}C]Loperamide as highly sensitive PET probe for measuring changes in P-glycoprotein functionallity [symposium abstract]. *J. Labelled Cpd. Radiopharm.*, **2003**, *46* (Supplement 1), S94.
[7]Passchier, J.; Comley, R.; Salinas, C.; Rabiner, E.; Gunn, R.; Cunningham, V.; Wilson, A.; Houle, S.; Gee, A.; Laruelle, M., Blood brain barrier permeability of [^{11}C]loperamide in humans under normal and impaired P-glycoprotein function [symposium abstract]. *J. Nucl.Med.*, **2008**, *49* (Supplement 1), 211P.

[^{11}C]-*N*-desmethyl loperamide was blood flow dependent under conditions of Pgp blockade [94]. Correction for regional cerebral blood flow measured with [^{15}O]H_2O PET revealed an uniform activity distribution pattern suggesting absence of regional differences in Pgp function in the monkey brain [94]. These results were later on confirmed in the human brain either with [^{11}C]-*N*-desmethyl loperamide and tariquidar as the Pgp inhibitor [82] or with other radiotracers (either (*R*)-[^{11}C]verapamil in combination with tariquidar [80] or *rac*-[^{11}C]verapamil and CsA [81]). Radio-HPLC analysis of mouse brain after injection of [^{11}C]-*N*-desmethyl loperamide showed that radiometabolites of [^{11}C]-*N*-desmethyl loperamide were also taken up into brain tissue: 43.6 and 91.3% of total radioactivity were in the form of unchanged [^{11}C]-*N*-desmethyl loperamide in wild-type and *Abcb1a*$^{-/-}$ / *Abcb1b*$^{-/-}$ mouse brain, respectively [93]. In addition, one radiometabolite, which was later on identified as the corresponding *N*-hydroxymethyl analogue [96], appeared to be also a Pgp substrate as indicated by 8-fold higher concentration levels in *Abcb1a*$^{-/-}$ /*Abcb1b*$^{-/-}$ compared to wild-type mouse brain. Therefore, similar to (*R*)-[^{11}C]verapamil, accurate quantification of cerebral Pgp function with [^{11}C]-*N*-desmethyl loperamide is compromised by the contamination of the brain PET signal with radiolabelled metabolites. Brain uptake in baseline scans is about 2-fold lower for [^{11}C]-*N*-desmethyl loperamide [82] than for (*R*)-[^{11}C]verapamil [59], which makes it even more difficult to assess regional cerebral Pgp function, without employing a Pgp inhibitor, with this radiotracer.

[^{11}C]Carvedilol

Carvedilol is a non-selective beta-antagonist with nanomolar affinity to beta-adrenoceptors. [^{11}C]Carvedilol was initially developed as a PET tracer for cerebral beta-adrenoceptor imaging, which was abandoned due to low brain uptake of the molecule [97]. [^{11}C]Carvedilol was then suggested as an alternative tracer to *rac*-[^{11}C]verapamil for imaging of Pgp function at the BBB, as it was shown to inhibit Pgp in vitro [98] and as it possesses a log *P* value of 2.0 which is more in the ideal range for brain PET tracers (0.9-2.5) than that of *rac*-[^{11}C]verapamil (log *P* 3.8) [99]. [^{11}C]Carvedilol was tested in rats, which showed low V_T values at baseline (0.4), which increased dose-dependently up to three-fold after CsA administration at doses from 0-50 mg/kg [99]. As lower CsA doses were needed to achieve maximum increase in brain V_T as compared to *rac*-[^{11}C]verapamil it was suggested that [^{11}C]carvedilol might be more sensitive to visualize cerebral Pgp function than *rac*-[^{11}C]verapamil. However, no further studies with [^{11}C]carvedilol have appeared in the literature since its first description as a Pgp substrate radiotracer in 2005.

[^{11}C]Colchicine

Colchicine, a tubulin-binding alkaloid of *Colchicum autumnale*, was ^{11}C-labelled by reacting desmethyl-colchicine with [^{11}C]CH_3I [100].[^{11}C]Colchicine was assessed in nude rats xenografted with a colchicine-sensitive and a colchicine-resistant strain of the human neuroblastoma BE (2)-C cell line [100]. PET imaging showed that tumoral activity uptake was generally low, but about 2-times lower in resistant than in sensitive tumors, consistent with Pgp-mediated efflux of the radiotracer in resistant tumors.

[^{11}C]Daunorubicin

The cytostatic agent daunorubicin was ^{11}C-labelled in low radiochemical yield (3±1%) in a 2-step radiosynthesis by reacting aldehyde precursor, in which the amino function was protected by a trifluoroacetic group, with [^{11}C]diazomethane, followed by alkaline hydrolysis of the protecting group [54]. In vitro experiments were performed with [^{11}C]daunorubicin in a human ovarian carcinoma cell line and its adriamycin resistant counterpart revealing 16-fold lower radioactivity accumulation in the resistant cell line, which could be raised to similar levels as in the sensitive cell line by addition of 50 μM verapamil. Furthermore Hendrikse and co-workers performed biodistribution experiments

with [^{11}C]daunorubicin in rats bearing tumors bilaterally, a Pgp negative small cell lung carcinoma (GLC_4) and its Pgp-overexpressing subline (GLC_4/Pgp) [55]. It could be shown that [^{11}C]daunorubicin accumulation was higher (159%) in the Pgp deficient compared to the Pgp-overexpressing tumor and that pretreatment of rats with CsA (50 mg/kg) raised the radioactivity level in GLC_4/Pgp tumors to the level of GLC_4 tumors.

[^{11}C]Docetaxel

The cytotoxic agent docetaxel, which belongs to the class of the taxanes, was ^{11}C-labelled in the BOC moiety of the molecule by reacting the corresponding primary amine with [^{11}C]*tert*-butyl-1,2,2,2-tetrachloroethyl carbonate in the presence of pyridine [101]. The synthesis was later on improved to produce the radiotracer in good manufacturing practice (GMP) quality for human applications [102]. [^{11}C]Docetaxel has recently been evaluated in patients with advanced solid tumors by performing whole-body PET/CT-scans [103]. No radiometabolites of [^{11}C]docetaxel were observed in plasma during the time course of the PET experiment by using radio-HPLC analysis. Moderate radioactivity uptake was observed in tumors, and shown to vary strongly between different tumors. High radioactivity uptake in the abdominal and pelvic region will in all likelihood preclude visualization of tumor masses located in these parts of the body.

[^{11}C]Gefitinib

Gefitinib, a selective inhibitor of epidermal growth factor receptor (EGFR) tyrosine kinase, was ^{11}C-labelled by *O*-methylation of its phenol precursor with [^{11}C]methyl triflate [104-105]. PET experiments with [^{11}C]gefitinib showed an 8 times higher brain activity uptake in *Abcb1a*$^{-/-}$ /*Abcb1b*$^{-/-}$ /*Abcg2*$^{-/-}$ than in wild-type mice [104]. Combined with the observation that pretreatment of wild-type mice with the dual Pgp/BCRP inhibitor elacridar (50 mg/kg) or with CsA (50 mg/kg) increased brain activity uptake of [^{11}C]gefitinib by 10.6 and 3.6 fold, respectively, it was concluded that [^{11}C]gefitinib was transported by Bcrp1 and Pgp at the murine BBB. However, as no BCRP-specific inhibitor was used, the selectivity of [^{11}C]gefitinib for Bcrp1 over Pgp could not be addressed.

[^{18}F]MPPF

[^{18}F]MPPF (4-(2′-methoxyphenyl)-1-[2′-(*N*-2′′-pyridinyl)-*p*-[^{18}F]fluorobenzamido] ethylpiperazine) was developed as a specific 5-HT_{1A} receptor antagonist and has been suggested to be a Pgp substrate. Cerebral uptake of [^{18}F]MPPF in rats was shown to be increased following administration of CsA [106-107] or tariquidar [108-109]. Moreover, brain activity uptake of [^{18}F]MPPF was shown to be 2 to 3 times higher in *Abcb1a*$^{-/-}$ compared to wild-type mice [106]. Bartmann and co-workers reported in a chronic rat model with spontaneous recurrent seizures that hippocampal K_1 increases of [^{18}F]MPPF following tariquidar challenge (15 mg/kg, i.v.) were lower in animals which responded to phenobarbital therapy as compared to non-responders, which was attributed to increased Pgp activity in non-responders [109]. However, interpretation of these data is complicated by the fact that [^{18}F]MPPF binds to cerebral 5-HT_{1A} receptors, which show decreased density in epileptic brain regions. In human patients with temporal lobe epilepsy a major reduction of the binding potential of [^{18}F]MPPF for 5-HT_{1A} receptors in the epileptogenic focus has been demonstrated which, when compared to the contralateral side, was greater than that seen with other PET tracers for 5-HT_{1A} receptors, possibly indicating Pgp action [110]. However, recently presented in vitro transport experiments in human Pgp overexpressing cells (MDCKII-hMDR1) using bidirectional transport and concentration equilibrium assays suggest that while [^{18}F]MPPF may be a Pgp substrate in rodents it is not transported by human Pgp,[8] which casts some doubt on the hypothesis that regional differences in [^{18}F]MPPF uptake seen in brains of human epilepsy patients were indeed mediated by Pgp efflux.

Radiolabelled paclitaxel and derivatives

Paclitaxel is as a natural chemotherapeutic agent (a taxane) derived from the yew tree *Taxus brevifolia* that triggers the arrest of cells in the G2/M cell cycle phase. It shows cytostatic potential in a wide range of common cancer types. Experiments in *Abcb1a*$^{-/-}$ /*Abcb1b*$^{-/-}$ mice indicated that paclitaxel is a Pgp substrate [111]. Although clinical evidence is somewhat conflicting some studies have reported an association of tumoral Pgp expression levels and clinical response of tumor patients to paclitaxel treatment [112]. [^{11}C]Paclitaxel was synthesized by labelling the corresponding primary amine precursor with [^{11}C]benzoyl chloride [113]. Apart from [^{11}C]paclitaxel, the molecule has also been labelled with ^{123}I [114], ^{124}I [115], ^{76}Br [115], ^{111}In [116] and ^{18}F [115]. Most in vivo data of all radiolabelled paclitaxel derivatives is available for 4-[^{18}F]fluoropaclitaxel, which was synthesized similar to the [^{11}C]tracer using the primary amine precursor by acylation with 4-[^{18}F]fluorobenzoylchloride or 4-[^{18}F]fluorobenzoic acid [115, 117]. Biodistribution studies with 4-[^{18}F]fluoropaclitaxel showed significantly increased activity uptake in heart (+79%), lung (+143%) and brain (+1400%) of *Abcb1a*$^{-/-}$ /*Abcb1b*$^{-/-}$ compared to wild-type mice [115]. However, intraperitoneal administration of tariquidar (10 mg/kg) at 5 min before 4-[^{18}F]fluoropaclitaxel injection was not able to significantly increase brain activity uptake in wild-type mice, to the same levels as in *Abcb1a*$^{-/-}$ /*Abcb1b*$^{-/-}$ mice [115]. A possible explanation for this could be that the employed tariquidar dose was too low and/or that the time span between tariquidar administration and injection of radiotracer was too short to achieve effective Pgp inhibition. Paired 4-[^{18}F]fluoropaclitaxel PET scans before and after i.v. administration of tariquidar (2 mg/kg) and arterial blood sampling were performed in rhesus monkeys [118]. Tariquidar was found to increase V_T, derived from Logan analysis, in liver (+104%) and lung (+87%), but not in brain. Gangloff and co-workers studied the biodistribution of 4-[^{18}F]fluoropaclitaxel in nude mice xenografted with human MCF-7 breast cancer cells and showed that tumoral activity uptake was doubled after administration of CsA (10 mg/kg, i.p.) [119]. In a follow-up study, 4-[^{18}F]fluoropaclitaxel distribution was studied with small-animal PET in nude mice xenografted with either MCF-7 cells or MCF-5/AdrR cells, an intrinsically paclitaxel-resistant cell line [120]. After PET imaging, mice were treated with a single dose of paclitaxel. It could be shown that mice with tumors that did not respond to paclitaxel treatment had lower tumoral activity uptake than mice with paclitaxel-sensitive tumors indicating that low 4-[^{18}F]fluoropaclitaxel uptake might serve as a predictor of chemoresistance [120]. Kurdziel *et al.* further studied 4-[^{18}F]fluoropaclitaxel distribution in nude mice xenografted on the right and left shoulder with two different KB epidermal carcinoma cell sublines, drug sensitive non-Pgp expressing KB 3-1 and drug-resistant Pgp expressing KB 8-5 cells [23]. Whereas PET imaging showed only small differences between resistant and sensitive tumors, ex vivo counting of excised tumors revealed a 3.2 fold higher activity content in KB 3-1 compared to KB 8-5 tumors.

[^{11}C]Phenytoin

Several lines of evidence suggest that the widely used antiepileptic drug phenytoin is a substrate of rodent and human Pgp [121-123] as well as rodent Mrp2 [124]. Phenytoin has been radiolabelled with ^{11}C starting from H[^{11}C]CN as early as 1978, which was in fact before clinical PET cameras have become available [125]. An alternative synthesis pathway making use of [^{11}C]phosgene was described later [126]. Scintigraphic imaging of [^{11}C]phenytoin was performed in rhesus monkeys showing measurable and persistent radioactivity uptake in brain, lung and liver [125]. Cerebral pharmacokinetics of [^{11}C]phenytoin were assessed in 8 patients with medically resistant partial epilepsy and 2 patients without epilepsy [127]. At steady-state, brain-to-blood ^{11}C-activity concentration

[8]Tournier, N.; Valette, H.; Goutal., S.; Schollhorn, M.; Saba, W.; Cisternino, S.; Scherrmann, J.; Bottlaender, M., Is [^{18}F]-pMPPF a P-glycoprotein substrate in human? [symposium abstract]. *Eur. J. Nucl. Med. Mol. Imaging*, **2010**, *37* (Supplement 2), S210.

ratios were determined for the visual cortex, resulting in an average value of 1.32 (range 1.05-1.66) in epilepsy patients compared to 1.61 (1.34-1.87) in nonepileptic patients. Whether [^{11}C]phenytoin steady-state concentration is lower within the epileptic focus was not addressed in this study. Preliminary data indicated that [^{11}C]phenytoin kinetics within the estimated epileptogenic area were not significantly different when compared to the contralateral homologous brain region in the same epilepsy patients [127], but clearly data from a modern high-resolution PET system are needed for such an analysis. PET tracers based on antiepileptic drugs, such as [^{11}C]phenytoin or [^{11}C]phenobarbital, which are only weak Pgp substrates, possess higher brain uptake than the high-affinity Pgp substrates (*R*)-[^{11}C]verapamil or [^{11}C]-*N*-desmethyl loperamide and are therefore expected to be better suited to assess regional differences in Pgp function in the epileptic brain.

[^{99m}Tc]Sestamibi

[^{99m}Tc]Sestamibi, a cationic radiotracer originally developed for myocardial scintigraphy, is a Pgp substrate and has been used to examine Pgp functional activity in vitro and in vivo under pathologic conditions [22, 25, 128]. In vitro studies in Chinese hamster cell lines showed decreasing intracellular concentrations of [^{99m}Tc]sestamibi with increasing Pgp expression levels [128]. Reversal of this effect could be shown by administration of Pgp inhibitors such as verapamil and CsA. Brain uptake of [^{99m}Tc]sestamibi was 4-fold higher in Pgp knockout than in wild-type mice [128]. [^{99m}Tc]Sestamibi is widely used to detect in vivo Pgp activity in tumors [129-130], and may be a useful technique for monitoring the development of Pgp-mediated multidrug resistance [25]. In rats, inflammation-mediated downregulation of brain *mdr1a* mRNA, the gene encoding Pgp in brain capillary endothelial cells in rodents, is associated with higher accumulation of [^{99m}Tc]sestamibi in the brain, further demonstrating the potential utility of [^{99m}Tc]sestamibi for noninvasively assessing Pgp function in vivo [131]. However, to a lesser extent, [^{99m}Tc]sestamibi is also transported by MRP1, which may form a bias for results obtained with [^{99m}Tc]sestamibi [132]. A series of clinical trials of Pgp inhibitors in cancer patients have used [^{99m}Tc]sestamibi and SPECT imaging as a surrogate marker of tumoral Pgp inhibition [133-135]. Due to the limitations of planar imaging to accurately quantify tumoral uptake of [^{99m}Tc]sestamibi, [^{94m}Tc]sestamibi has been developed as a PET version of this radiotracer [136]. Alternative Pgp substrates for SPECT imaging are [^{99m}Tc]tetrofosmin [137] as well as several other metalloorganic complexes [25].

Miscellaneous compounds

Van Waarde and co-workers recently reported the ^{11}C-labelling and in vivo evaluation of the Pgp substrate 6,7-dimethoxy-2-[3-(5-methoxy-1,2,3,4-tetrahydronaphthalen-1-yl)-propyl]-1,2,3,4-tetrahydro-isoquinoline (MC266) [138]. Cerebral V_T of [^{11}C]MC266 in rats was about 3 times higher than that of *rac*-[^{11}C]verapamil. Pretreatment of rats with CsA (50 mg/kg, i.v.) increased cerebral V_T by 2.8 fold compared to baseline scans. [^{11}C]MC266 could be an interesting alternative Pgp substrate radiotracer to [^{11}C]verapamil or [^{11}C]-*N*-desmethyl loperamide as it might facilitate the mapping of regional differences in cerebral Pgp function in epilepsy by virtue of its higher brain uptake. De Bruyne and co-workers labelled the Pgp modulator 6,7-dimethoxy-2-(6-methoxy-naphthalen-2-ylmethyl)-1,2,3,4-tetrahydroisoquinoline (MC80) with ^{11}C [139]. Biodistribution studies with [^{11}C]MC80 in wild-type (FVB) mice demonstrated a high baseline brain uptake (7.66±1.38%ID/g at 1 min post injection, p.i.). Cerebral activity concentration was moderately increased (2-fold) in wild-type mice after CsA pretreatment (50 mg/kg) as well as in *Abcb1a*$^{-/-}$/*Abcb1b*$^{-/-}$ mice, suggesting the compound to be a weak Pgp substrate [139].

Apart from the aforementioned radiotracers, brain uptake of several other PET ligands, which were developed for other purposes than ABC transporter imaging, was found to be

modulated by Pgp and related transporters at the BBB. These include but are not limited to the central benzodiazepine receptor ligand [^{11}C]flumazenil [140], the adenosine A_{2A} receptor ligand [^{11}C]TMSX [140], the adenosine A_1 receptor ligand [^{11}C]MPDX [140], the acetyl cholinesterase tracer [^{11}C]donepezil [140], the beta-adrenoceptor ligands *(S)*-[^{18}F]fluorocarazolol and [^{11}C]carazolol [141], the dopamine D_3 receptor ligand [^{11}C]GR218231 [142], the 5-HT_{1A} receptor ligand [^{11}C](*R*)-(-)-RWAY [143] and the dopamine transporter tracer 4-(2-(bis(4-fluorophenylmethoxy)ethyl)-1-(4-[^{123}I]iodobenzyl)piperidine ([^{123}I]FMIP) [144]. This extensive list underlines the broad substrate specificity of cerebral multidrug transporters and suggests that Pgp efflux affinity should be taken into account as an additional parameter when developing PET tracers targeted to the CNS, just as it is usually done in CNS drug development [18].

RADIOLABELLED PGP INHIBITORS

The low brain uptake of most radiolabelled Pgp substrates, in particular that of (*R*)-[^{11}C]verapamil and [^{11}C]-*N*-desmethyl loperamide, makes them unsuitable to study regional differences in Pgp function in the brain. This is because regionally increased Pgp function as it is expected to occur in therapy refractory epilepsy would lead to a further reduction of the signal which is very difficult to detect against an already low background of radiotracer uptake. Therefore several research groups have started to develop PET tracers based on Pgp inhibitors, which are expected to bind to Pgp without being transported and allow for the visualization of Pgp expression levels, in analogy to PET tracers which are commonly used for mapping the distribution of other transporter proteins in brain, such as [^{11}C]-labelled 2-beta-carbomethoxy-3beta-(4-fluorophenyl)-tropane ([^{11}C]CFT) for the dopamine transporter [145] or [^{11}C]3-amino-4-(2-dimethylaminomethyl-phenylsulfanyl)-benzonitrile ([^{11}C]DASB) for the serotonin transporter [146]. A Pgp inhibitor radiotracer should give a signal increase rather than a decrease (as will a Pgp substrate tracer) in brain regions that overexpress Pgp and therefore allow for assessing differences in Pgp expression in different brain regions (e.g. epileptic versus non-epileptic brain regions).

Four radiotracers based on third-generation Pgp inhibitors have been reported to date: [^{11}C]laniquidar [147], [^{11}C]elacridar [148-149], [^{11}C]tariquidar [150-151] and the elacridar derivative [^{11}C]MC18 (6,7-dimethoxy-2-{3-[4-methoxy-3,4-dihydro-2H-naphthalen-(1E)-ylidene]-propyl}-1,2,3,4-tetrahydro-isoquinoline) [138]. Elacridar, tariquidar and MC18 were ^{11}C-labelled by [^{11}C]methylation of phenolic hydroxyl groups with [^{11}C]CH_3 I or [^{11}C]methyl triflate and [^{11}C]laniquidar [147] was synthesized by converting the corresponding carboxylic acid precursor into its [^{11}C]methyl ester. [^{11}C]Tariquidar has been synthesized by two different research groups, but in different labelling positions (either the dimethoxy-tetrahydroisoquinolinylethyl [151] or the anthranilic acid moiety [150]).

Unexpectedly, in vivo experiments in rats and mice showed that [^{11}C]laniquidar, [^{11}C]elacridar and [^{11}C]tariquidar possessed very low brain uptake (<0.5 SUV), which was several-fold increased after administration of unlabelled inhibitor. For instance, brain uptake of [^{11}C]elacridar in rats was 5.4 times increased relative to baseline scans after administration of elacridar (5 mg/kg, i.v.) [148]. For [^{11}C]tariquidar, brain activity uptake in rats was 2.9 and 4.3 times higher after i.v. injection of tariquidar (15 mg/kg) and elacridar (5 mg/kg), respectively [150]. Interestingly, for [^{11}C]laniquidar brain activity uptake in rats was 6 to 9 times higher in different brain regions after administration of CsA (50 mg/kg, i.v.), whereas no effect on cerebral activity uptake was seen after pretreatment with valspodar (20 mg/kg, i.p.) [147]. The only tracer which showed different behavior was [^{11}C]MC18, which had about three-fold higher brain activity uptake in baseline scans than the other [^{11}C]inhibitors (peak brain uptake in rat brain approximately 1.5 SUV) [138]. In addition, whole-brain V_T of [^{11}C]MC18 was reduced by approximately 30% after

pretreatment with unlabelled MC18 (15 mg/kg), which is, however, by itself no sufficient proof that [^{11}C]MC18 indeed binds to cerebral Pgp [138]. To prove Pgp-specific binding of [^{11}C]MC18 additional studies involving administration of Pgp inhibitors such as CsA, elacridar or tariquidar need to be performed. Apart from rats, [^{11}C]elacridar and [^{11}C]tariquidar were also tested in wild-type and transporter knockout mice, which revealed low brain uptake in wild-type animals and increased uptake values in transporter knockout animals with the rank order *Abcb1a*$^{-/-}$ /*Abcb1b*$^{-/-}$ /*Abcg2*$^{-/-}$ >> *Abcb1a*$^{-/-}$ /*Abcb1b*$^{-/-}$ > *Abcg2*$^{-/-}$ [148-151]. In *Abcb1a*$^{-/-}$ /*Abcb1b*$^{-/-}$/*Abcg2*$^{-/-}$ mice, brain concentrations of [^{11}C]elacridar [149] and [^{11}C]tariquidar [150-151] were 8 to 9-fold higher as compared to wild-type animals. Kawamura and co-workers found dose-dependent increases of brain-to-blood activity ratios in wild type mice when increasing doses of unlabelled compound were added to the radiotracer with ED_{50} values of 4.4 and 1.55 mg/kg for [^{11}C]tariquidar and [^{11}C]elacridar, respectively [149, 151]. In comparison to the Pgp substrate radiotracers (*R*)-[^{11}C]verapamil and [^{11}C]-*N*-desmethyl loperamide, [^{11}C]laniquidar, [^{11}C]elacridar and [^{11}C]tariquidar showed remarkable metabolic stability. At 20 min after radiotracer injection into rats, 85 and 96% of total radioactivity in plasma were in the form of unchanged parent tracer for [^{11}C]elacridar and [^{11}C]tariquidar, respectively [148, 150]. For [^{11}C]laniquidar, 68% unchanged parent was found in rat plasma at 30 min after tracer injection [147]. Kawamura and colleagues found that 95.4 and 92.2% of total radioactivity in wild-type mouse brain was in the form of unchanged parent at 30 min after tracer injection, for [^{11}C]elacridar and [^{11}C]tariquidar, respectively [149, 151]. For [^{11}C]MC18 no metabolism data were reported. Bauer and colleagues performed in vitro autoradiography with [^{11}C]tariquidar and found significantly decreased binding in *Abcb1a*$^{-/-}$/*Abcb1b*$^{-/-}$, *Abcg2*$^{-/-}$ and *Abcb1a*$^{-/-}$/*Abcb1b*$^{-/-}$/*Abcg2*$^{-/-}$ as compared to wild-type mouse brain [150]. Moreover, co-incubation with elacridar (1 μM) significantly reduced binding in wild-type mice but not in *Abcg2*$^{-/-}$ and *Abcb1a*$^{-/-}$ /*Abcb1b*$^{-/-}$ /*Abcg2*$^{-/-}$ mouse brain. Yamasaki *et al.* studied [^{11}C]elacridar distribution in nude mice xenografted with human colon adenocarcinoma (Caco-2) cells, which were expressing both Pgp and BCRP as shown by Western blot analysis [152]. They found that tumoral uptake of activity was low (0.2 SUV) and increased by 1.8 fold after i.v. administration of elacridar (5 mg/kg) [152]. Kawamura *et al.* have very recently reported the synthesis of *O*-[^{18}F]fluoroethyl analogues of elacridar and tariquidar and shown that they behaved in vivo in rodents similarly to [^{11}C]elacridar and [^{11}C]tariquidar [153].

Taken together all in vivo data reported so far with [^{11}C]laniquidar, [^{11}C]elacridar and [^{11}C]tariquidar suggested that these radiotracers are transported by Pgp and/or BCRP at the BBB. This comes somewhat as a surprise as these molecules were developed as non-transported Pgp inhibitors and there is data available in the literature to support this. According to Polli *et al.* the criteria for classifying a compound as a non-transported Pgp inhibitor are (i) a basolateral-apical (B-A) to apical-basolateral (A-B) concentration ratio <2 in monolayer transport assays, (ii) lack of adenosine triphosphatase (ATPase) activity stimulation and (iii) inhibition of substrate transport [154]. At least elacridar [154-155] and tariquidar [156-158] seem to meet all three criteria. However, very recent data suggest that tariquidar is at low concentrations an avid substrate of BCRP [159]. Kannan and co-workers found that accumulation of ^{3}H-labelled tariquidar (1 nM) was several fold-lower in a cell line overexpressing human BCRP relative to the parental cell line and increased to similar levels as in parental cells after co-incubation with the BCRP inhibitor fumitremorgin C, which was consistent with BCRP transport of tariquidar [159]. On the other hand, when a cell line which overexpressed human Pgp, was incubated with [^{3}H]tariquidar, cellular uptake was higher relative to parental cells, which pointed to binding of [^{3}H]tariquidar to Pgp [159]. Moreover, it was shown that tariquidar dose-dependently stimulated BCRP ATPase activity in membrane vesicles to 2.5-fold the basal activity, further demonstrating a direct substrate interaction with BCRP [159]. Given these recent data and the close structural

similarity between elacridar and tariquidar it seems very likely that the substrate-like in vivo behavior of [^{11}C]tariquidar and [^{11}C]elacridar was caused by BCRP transport at the BBB. This is also in line with the observation that unlabelled elacridar, which is a more potent BCRP inhibitor than tariquidar [40], increased brain activity uptake of [^{11}C]tariquidar in rats to a greater extent than unlabelled tariquidar [150]. Moreover, the observation that CsA increased brain uptake of [^{11}C]laniquidar in rats whereas valspodar did not might be explained by the fact that CsA inhibits BCRP [160] and valspodar does not [161].

So if [^{3}H]tariquidar binds in vitro to Pgp while it is transported by BCRP, what is the reason that PET experiments with [^{11}C]tariquidar in Bcrp1-knockout mice gave an almost equally low brain signal as in wild-type mice [150-151]? There are two possible explanations for this. First, in vivo [^{11}C]tariquidar seems to be not only transported by Bcrp1 but also by Pgp at the rodent BBB, which efficiently keeps the radiotracer out of brain tissue when Bcrp1 is knocked out. Second, the Pgp binding affinity of tariquidar may not be high enough in relation to the density (B_{max}) of Pgp at the BBB to obtain a Pgp-specific PET signal. Kamiie and colleagues report a B_{max} of the Mdr1a peptide of 15 fmol/μg protein in mouse brain capillaries, which translates to a value of 1.5 nM when assuming that the BBB constitutes only about 0.1% of total brain weight and that the protein content of brain capillaries is approximately 10% [34]. The ratio of the B_{max} of a given target protein to the equilibrium dissociation constant (K_D) of a prospective radioligand is commonly used as a predictor of the target-to-nontarget ratio to be expected for in vivo imaging [162]. Based on a K_D value for binding of [^{3}H]tariquidar to Chinese hamster ovary resistant cells (CHrB30) of 5.1 nM [156], the B_{max}/K_D is approximately 0.3 for tariquidar, which is in all likelihood too low to visualize Pgp at the BBB with [^{11}C]tariquidar. Therefore, in the search for improved Pgp inhibitors to visualize Pgp at the BBB compounds should be used which have an at least 10-fold lower K_D than tariquidar.

BCRP RADIOTRACERS

In contrast to the wealth of compounds that has been developed to visualize Pgp in vivo, only very few BCRP tracers have been reported to date. The most challenging aspect in the development of BCRP selective radiotracers is the substantial overlap in substrate specificity with Pgp [37]. An interesting candidate compound for the development of a BCRP-selective substrate radiotracer is the muscle relaxant dantrolene, which has only very recently been described as a specific BCRP substrate [163]. Data in transporter knockout mice show that the brain-to-blood ratio of dantrolene ($K_{p,brain}$) is significantly greater (about 3-fold) in *Abcg2*$^{-/-}$ and *Abcb1a*$^{-/-}$/*Abcb1b*$^{-/-}$/*Abcg2*$^{-/-}$ mice than in wild-type mice, whereas no differences were seen between wild-type and *Abcb1a*$^{-/-}$/*Abcb1b*$^{-/-}$ mice, which gives strong support for Bcrp1 over Pgp in vivo selectivity of dantrolene [164]. Recently the synthesis of [^{11}C]dantrolene has been reported based on [^{11}C]phosgene as a labelling agent [165]. However, no in vivo data of [^{11}C]dantrolene have been reported to date.

The potent third-generation Pgp inhibitors tariquidar and elacridar are also able to inhibit BCRP, but at higher concentrations than those at which they inhibit Pgp [40]. It has recently been discovered that structural modifications at the benzamide core of tariquidar result in potent and selective BCRP inhibitors [40]. Out of a series of 10 tariquidar-like compounds, methyl 4-((4-(2-(6,7-dimethoxy-1,2,3,4-tetrahydroisoquinolin-2-yl)ethyl)phenyl)amino-carbonyl)-2-(quinoline-2-carbonylamino)benzoate was identified as a potent BCRP inhibitor, which inhibits BCRP-mediated transport of mitoxantrone in topotecan-resistant MCF-7 breast cancer cells with a half-maximum inhibitory concentration (IC_{50}) of 60 nM and displays approximately 500-fold selectivity for inhibition of BCRP over Pgp [40]. This compound has been labelled with ^{11}C by two different research groups by reaction of the corresponding carboxylic acid precursor with [^{11}C]methyl triflate [166-167]. Whereas Wang

reported no in vivo evaluation of the compound [167], Mairinger *et al.* characterized the compound with small-animal PET imaging in wild-type and *Abcb1a*$^{-/-}$ /*Abcb1b*$^{-/-}$, *Abcg2*$^{-/-}$ and *Abcb1a*$^{-/-}$/*Abcb1b*$^{-/-}$/*Abcg2*$^{-/-}$ mice [166]. The in vivo behavior of [^{11}C]methyl 4-((4-(2-(6,7-dimethoxy-1,2,3,4-tetrahydroisoquinolin-2-yl)ethyl)phenyl)amino-carbonyl)-2-(quinoline-2-carbonylamino)benzoate was more in line with a dual Pgp and BCRP substrate than a BCRP-selective inhibitor as indicated by 4.8-and 10.3-fold higher brain-to-plasma ratios in *Abcb1a*$^{-/-}$ /*Abcb1b*$^{-/-}$ and *Abcb1a*$^{-/-}$ / *Abcb1b*$^{-/-}$ /*Abcg2*$^{-/-}$ mice, respectively, as compared to wild-type animals, but only modestly increased ratios in *Abcg2*$^{-/-}$ mice [166]. The observation that the combined effect of Pgp and Bcrp1 knockout (*Abcb1a*$^{-/-}$ /*Abcb1b*$^{-/-}$ /*Abcg2*$^{-/-}$ mice) on brain uptake of radiotracer was far greater than the sum of its individual contributions in *Abcb1a*$^{-/-}$ / *Abcb1b*$^{-/-}$ and *Abcg2*$^{-/-}$ mice has also been made for [^{11}C]elacridar [149] and [^{11}C]tariquidar [150-151] and gives evidence of the concerted action of Pgp and BCRP in the BBB [168-169]. In the absence of Pgp, BCRP may take over its role in limiting brain entry of dual substrates and vice versa. These results emphasize the difficulties in predicting the in vivo behavior of ABC transporter ligands based on in vitro data and underline the importance of performing in vivo experiments as early as possible in the rational design of PET ligands for ABC transporters [166].

MRP RADIOTRACERS

For imaging of MRP relatively few radiotracers have been reported so far. As MRP2 plays an important role in transporting glutathione-, glucuronide- or sulfate-conjugated drugs from hepatocytes into the bile canaliculus, MRP imaging probes have been used to assess hepatobiliary transport. For instance, the inflammatory cytokine leukotriene C4 (LTC_4) and its metabolites LTD_4 and LTE_4 have been shown to be substrates for both MRP1 and MRP2 [26]. *N*-[^{11}C]acetyl-LTE_4 [170] was examined in normal rats and in Mrp2-deficient GY/TR$^-$ rats using PET [171]. It was shown that in GY/TR$^-$ rats there was a reduced clearance of radioactivity from the liver and negligible amounts of radioactivity in the intestine compared with normal rats, suggesting that *N*-[^{11}C]acetyl-LTE_4 might be useful for visualization of hepatic MRP2 and possibly MRP1. Hendrikse showed that the cholescintigraphic agent [^{99m}Tc]*N*-(2,6-dimethylphenylcarbamoylmethyl)-iminodiacetic acid ([^{99m}Tc]disofenin) is transported by MRP1 in vitro [172]. Planar imaging experiments in control rats and GY/TR$^-$ rats showed that the clearance of radioactivity from the liver was considerably faster in control (half-life: 7±9 min) than in GY/TR$^-$ rats (half-life: 40±9 min) which was consistent with hepatobiliary MRP2 transport of this radiotracer [172]. Similarly, Bhargava *et al.* showed that the hepatobiliary imaging agent [^{99m}Tc]*N*-[2-[(3-bromo-2,4,6-trimethylphenyl)amino]-2-oxoethyl]-*N*-(carboxymethyl)-glycine ([^{99m}Tc]mebrofenin) is mainly excreted by MRP2 into bile [173]. Mavel et al synthesized a series of halogen-substituted flavone derivatives as potential PET and SPECT ligands to visualize MRP1 [174]. In vitro experiments revealed that some of these compounds were able to enhance doxorubicin toxicity in hMRP1-expressing GLC_4/Adr cells, suggesting that these compounds were modulators of MRP1. However, neither the radiolabelling nor the in vivo characterization of any of these compounds has been reported to date. (15*R*)-16-*m*-[^{11}C]tolyl-17,18,19,20-tetranorisocarbacyclin methyl ester (15*R*-[^{11}C]TIC-Me) has been shown to allow for in vivo kinetic analysis of MRP2-mediated hepatobiliary transport [175]. In vivo, 15*R*-[^{11}C]TIC-Me is rapidly converted in blood into its acid form 15*R*-[^{11}C]TIC, which is in turn converted into at least three radiometabolites. Two of these radiometabolites were shown to be MRP2 substrates using an in vitro transport assay. PET evaluation in normal and Mrp2-deficient rats showed that at 90 min after injection of 15*R*-[^{11}C]TIC-Me, radioactivity levels in the bile of Mrp2-deficient rats were significantly reduced compared to control rats, which was shown to be caused by decreased canalicular efflux clearance of the Mrp2-transported radiometabolites of 15*R*-[^{11}C]TIC-Me [175].

Okamura *et al.* recently reported a highly novel and elegant strategy for quantitative imaging of MRP1 function in the brain based on the metabolite extrusion method, a kind of prodrug/drug approach [176]. This method relies on the use of a radiolabelled probe which readily enters the brain by passive diffusion after i.v. injection. While a portion of the incorporated compound diffuses back into the blood, the rest is efficiently converted into a hydrophilic radiometabolite that is then extruded by an efflux transporter of interest [26]. If passive diffusion of the hydrophilic radiometabolite across the BBB is negligible, the efflux rate constant of activity from brain will directly reflect efflux transporter activity. Glutathione (GSH) transferases (GSTs) are known to protect the brain from toxic compounds by formation of GSH conjugates, which in turn are expelled from the brain by MRP1 mediated efflux across the BBB. Okamura and colleagues used 6-bromo-7-[^{11}C]methylpurine as a PET tracer, which was shown to have high brain uptake in wild-type mice after i.v. administration (approximately 0.6% ID/g at 1.5 min p.i.) followed by a rapid wash-out with an efflux rate of 1.4 h^{-1}[176]. Conversely, in *Abcc1*$^{-/-}$ mice the efflux rate of activity after injection of 6-bromo-7-[^{11}C]methylpurine was only 0.15% h^{-1}, i.e. 90% lower than in wild-type animals suggesting the efflux rate as a quantitative measure of Mrp1 activity. Radio-HPLC analysis of brain extracts both from wild-type and *Abcc1*$^{-/-}$ mice had shown that within 15 min after injection of ^{14}C-labelled 6-bromo-7-methylpurine all activity was quantitatively converted into the corresponding GSH conjugate [176]. For a successful application of this approach to other species including humans it is critical that the conversion rate of the PET tracer into its GSH conjugate is equally fast as in rodents. As the activity of GST is susceptible to species differences, Okamura synthesized a series of 6-halogen-9-(or 7)-[^{14}C]methylpurines, and evaluated them in vitro with respect to enzymatic reactivity with GSH using brain homogenates from the mouse, rat, or monkey [177]. From this series of compounds, 6-fluoro-9-methylpurine emerged as promising candidate for human applications because it has a sufficiently high conversion rate by monkey GST and can be produced in higher radiochemical yield by ^{11}C-methylation than the 7-methyl isomer [26, 177]. Taken together, these data suggest that 6-bromo-7-[^{11}C]methylpurine PET is able to quantitatively determine Mrp1 function in the rodent brain. This method is very attractive as it overcomes the problem of low brain activity uptake associated with most other PET tracers, which have so far been described to measure ABC transporter function. Another advantage of this approach is that no arterial input function would be needed as the efflux rate constant as a quantitative parameter of transporter function can be directly derived from the brain time-activity curves. A possible limitation of this approach is that several processes other than MRP1 transport might contribute to the efflux of the radiolabelled GSH conjugate from brain into blood including enzymatic conversion or other active transport processes (for example by organic anion transporters and organic anion transporting polypeptides) and it is currently not known which of these is actually the rate-limiting step [26]. Translation of this approach to the imaging of other efflux transporters at the BBB, notably Pgp, would be of high interest. However, in contrast to MRP1, which is mainly expressed at the abluminal membrane of brain capillary endothelial cells, Pgp efflux pumps are primarily expressed on the luminal membrane. It is difficult to predict how the difference in location of these pumps will affect the applicability of the metabolite extrusion method to the imaging of Pgp. Another difficulty is related to the fact that in contrast to MRP1, Pgp transports lipophilic compounds. Therefore brain elimination of a lipophilic Pgp substrate formed in brain tissue from a non-Pgp substrate prodrug might occur both by passive diffusion and Pgp efflux.

CONCLUSION

We have reviewed PET and SPECT tracers to assess ABC transporter function and expression in vivo. A considerable challenge in the development of radiotracers for ABC transporters is the lack of candidate molecules which show selectivity for only one ABC transporter type. However, by using radiolabelled transporter substrates in combination with

unlabelled inhibitors and by carefully balancing the transporter selectivity profile of radiolabelled substrate against unlabelled inhibitor, the availability of purely selective radiotracers may not be mandatory.

The major focus for in vivo imaging of ABC transporters has so far been placed on Pgp located at the BBB and in solid tumors. A particularly promising application of an in vivo imaging method of Pgp could be in personalized medicine to identify epilepsy patients or cancer patients with increased Pgp function for applying altered treatment strategies, such as co-administration of a specific Pgp inhibitor. The most widely used Pgp substrate radiotracers for PET imaging are (*R*)-[^{11}C]verapamil and [^{11}C]-*N*-desmethyl loperamide. A drawback of these radiotracers is their low brain uptake, which hampers the mapping of regional differences in transporter function in the brain as they are expected to occur in epilepsy patients. Approaches to overcome this limitation include the performance of PET scans after half-maximum inhibition of Pgp with suitable inhibitors such as tariquidar, which has shown some promise in pilot studies[2,5], as well as the use of low-affinity transporter substrates, such as [^{18}F]MPPF, [^{11}C]phenytoin or [^{11}C]MC266. Another potentially powerful approach to overcome the problem of low brain PET signals obtained with Pgp substrate probes is the use of the metabolite extrusion method which has already been successfully applied to the imaging of cerebral MRP1 [176]. An important limitation of (*R*)-[^{11}C]verapamil or [^{11}C]-*N*-desmethyl loperamide is the significant brain uptake of radiolabelled metabolites, which confounds the measurement of cerebral Pgp function. Therefore the availability of Pgp substrate probes with better metabolic stability and absence of brain-penetrating radiometabolites would be of considerable interest. The development of Pgp inhibitor based PET tracers, such as ^{11}C-labelled laniquidar, elacridar and tariquidar, has so far been unsuccessful, as these radiotracers have failed to provide Pgp-specific brain PET signals, which was most likely caused by too low K_D values of these molecules in relation to the B_{max} of cerebral Pgp. In addition there is compelling evidence that ^{11}C-labelled laniquidar, elacridar and tariquidar are avid substrates of BCRP and possibly Pgp at the BBB [159], which underlines the importance of assessing the affinity of potential Pgp PET probes to other ABC transporters expressed at the BBB as well. An effective Pgp inhibitor PET ligand remains to be identified and should ideally lack efflux activity by BCRP and the MRPs and possess subnanomolar binding affinity to Pgp. Because in vitro transport experiments often fail to accurately predict the in vivo situation, researchers are encouraged to conduct in vivo experiments, for instance in wild-type and ABC transporter knockout mice [29], as early as possible in the rational design of ABC transporter imaging ligands. For other ABC transporters than Pgp, only very few PET and SPECT tracers have been described so far. It is hoped that the experience gained with the in vivo imaging of Pgp can be successfully applied in the future to the design of radioprobes to visualize other transport proteins such as BCRP or the MRPs.

Acknowledgments

The authors would like to thank the referees of this article for their thoughtful and constructive comments. The authors' own studies are funded by the Austrian Science Fund (FWF) project "Transmembrane Transporters in Health and Disease" (SFB F35) and by the European Community's Seventh Framework Programme (FP7/2007-2013) under grant agreement number 201380 ("EURIPIDES").

REFERENCES

[1]. Müller M, Schmid R, Georgopoulos A, Buxbaum A, Wasicek C, Eichler HG. Application of microdialysis to clinical pharmacokinetics in humans. Clin. Pharmacol. Ther. 1995; 57(4):371–380. [PubMed: 7712664]

[2]. Müller M, dela Peña A, Derendorf H. Issues in pharmacokinetics and pharmacodynamics of anti-infective agents. II: tissue distribution. Antimicrob. Agents Chemother. 2004; 48(5):1441–1453. [PubMed: 15105091]

[3]. Gottesman MM, Fojo T, Bates SE. Multidrug resistance in cancer: role of ATP-dependent transporters. Nat. Rev. Cancer. 2002; 2(1):48–58. [PubMed: 11902585]

[4]. Löscher W, Potschka H. Drug resistance in brain diseases and the role of drug efflux transporters. Nat. Rev. Neurosci. 2005; 6(8):591–602. [PubMed: 16025095]

[5]. Löscher W, Potschka H. Role of drug efflux transporters in the brain for drug disposition and treatment of brain diseases. Prog. Neurobiol. 2005; 76(1):22–76. [PubMed: 16011870]

[6]. Szakacs G, Paterson JK, Ludwig JA, Booth-Genthe C, Gottesman MM. Targeting multidrug resistance in cancer. Nat. Rev. Drug Discov. 2006; 5(3):219–234. [PubMed: 16518375]

[7]. Vautier S, Fernandez C. ABCB1: the role in Parkinson's disease and pharmacokinetics of antiparkinsonian drugs. Expert Opin. Drug Metab. Toxicol. 2009; 5(11):1349–1358. [PubMed: 19663741]

[8]. Jedlitschky G, Vogelgesang S, Kroemer HK. MDR1-P-glycoprotein (ABCB1)-mediated disposition of amyloid-beta peptides: implications for the pathogenesis and therapy of Alzheimer's disease. Clin. Pharmacol. Ther. 2010; 88(4):441–443. [PubMed: 20856238]

[9]. Ohtsuki S, Ito S, Terasaki T. Is P-glycoprotein involved in amyloid-beta elimination across the blood-brain barrier in Alzheimer's disease? Clin. Pharmacol. Ther. 2010; 88(4):443–445. [PubMed: 20856239]

[10]. Gomes CM, Abrunhosa AJ, Ramos P, Pauwels EK. Molecular imaging with SPECT as a tool for drug development. Adv. Drug Deliv. Rev. 2010 in press; DOI: 10.1016/j.addr.2010.09.015.

[11]. Langer O, Müller M. Methods to assess tissue-specific distribution and metabolism of drugs. Curr. Drug Metab. 2004; 5(6):463–481. [PubMed: 15578942]

[12]. Wagner CC, Langer O. Approaches using molecular imaging technology - use of PET in clinical microdose studies. Adv. Drug Deliv. Rev. 2010 in press; DOI: 10.1016/j.addr.2010.09.011.

[13]. Kjaer A. Molecular imaging of cancer using PET and SPECT. Adv. Exp. Med. Biol. 2006; 587:277–284. [PubMed: 17163171]

[14]. Smith SV. Challenges and opportunities for positron-emission tomography in personalized medicine. IDrugs. 2005; 8(10):827–833. [PubMed: 16254803]

[15]. Fox E, Bates SE. Tariquidar (XR9576): a P-glycoprotein drug efflux pump inhibitor. Expert Rev. Anticancer Ther. 2007; 7(4):447–459. [PubMed: 17428165]

[16]. Bates SF, Chen C, Robey R, Kang M, Figg WD, Fojo T. Reversal of multidrug resistance: lessons from clinical oncology. Novartis Found. Symp. 2002; 243:83–96. discussion 96-102, 180-185. [PubMed: 11990784]

[17]. Sisodiya SM, Bates SE. Treatment of drug resistance in epilepsy: one step at a time. Lancet Neurol. 2006; 5(5):380–381. [PubMed: 16632304]

[18]. Pike VW. PET radiotracers: crossing the blood-brain barrier and surviving metabolism. Trends Pharmacol. Sci. 2009; 30(8):431–440. [PubMed: 19616318]

[19]. Halldin C, Gulyás B, Langer O, Farde L. Brain radioligands - state of the art and new trends. Q. J. Nucl. Med. 2001; 45(2):139–152. [PubMed: 11476163]

[20]. Pike VW. Positron-emitting radioligands for studies *in vivo* - probes for human psychopharmacology. J. Psychopharmacol. (Oxf). 1993; 7(2):139–158.

[21]. Hendrikse NH, Vaalburg W. Imaging of P glycoprotein function in vivo with PET. Novartis Found. Symp. 2002; 243:137–45. discussion 145-148, 180-185. [PubMed: 11990773]

[22]. Kannan P, John C, Zoghbi SS, Halldin C, Gottesman MM, Innis RB, Hall MD. Imaging the function of P-glycoprotein with radiotracers: pharmacokinetics and in vivo applications. Clin. Pharmacol. Ther. 2009; 86(4):368–377. [PubMed: 19625998]

[23]. Kurdziel KA, Kalen JD, Hirsch JI, Wilson JD, Agarwal R, Barrett D, Bear HD, McCumiskey JF. Imaging multidrug resistance with 4-[^{18}F]fluoropaclitaxel. Nucl. Med. Biol. 2007; 34(7):823–831. [PubMed: 17921033]

[24]. Luurtsema G, Verbeek GL, Lubberink M, Lammertsma AA, Dierckx R, Elsinga P, Windhorst AD, van Waarde A. Carbon-11 labeled tracers for in vivo imaging P-glycoprotein function:

kinetics, advantages and disadvantages. Curr. Top. Med. Chem. 2010; 10(17):1820–1833. [PubMed: 20645915]

[25]. Sharma V. Radiopharmaceuticals for assessment of multidrug resistance P-glycoprotein-mediated drug transport activity. Bioconjug. Chem. 2004; 15(6):1464–1474. [PubMed: 15546216]

[26]. Okamura T, Kikuchi T, Irie T. PET imaging of MRP1 function in the living brain: method development and future perspectives. Curr. Top. Med. Chem. 2010; 10(17):1810–1819. [PubMed: 20645911]

[27]. Juliano RL, Ling V. A surface glycoprotein modulating drug permeability in Chinese hamster ovary cell mutants. Biochim. Biophys. Acta. 1976; 455(1):152–162. [PubMed: 990323]

[28]. Ambudkar SV, Kimchi-Sarfaty C, Sauna ZE, Gottesman MM. P-glycoprotein: from genomics to mechanism. Oncogene. 2003; 22(47):7468–7485. [PubMed: 14576852]

[29]. Lagas JS, Vlaming ML, Schinkel AH. Pharmacokinetic assessment of multiple ATP-binding cassette transporters: the power of combination knockout mice. Mol. Interv. 2009; 9(3):136–145. [PubMed: 19592674]

[30]. Litman T, Druley TE, Stein WD, Bates SE. From MDR to MXR: new understanding of multidrug resistance systems, their properties and clinical significance. Cell. Mol. Life Sci. 2001; 58(7):931–959. [PubMed: 11497241]

[31]. Doyle LA, Ross DD. Multidrug resistance mediated by the breast cancer resistance protein BCRP (ABCG2). Oncogene. 2003; 22(47):7340–7358. [PubMed: 14576842]

[32]. Robey RW, To KK, Polgar O, Dohse M, Fetsch P, Dean M, Bates SE. ABCG2: a perspective. Adv. Drug Deliv. Rev. 2009; 61(1):3–13. [PubMed: 19135109]

[33]. Polgar O, Robey RW, Bates SE. ABCG2: structure, function and role in drug response. Expert Opin. Drug Metab. Toxicol. 2008; 4(1):1–15. [PubMed: 18370855]

[34]. Kamiie J, Ohtsuki S, Iwase R, Ohmine K, Katsukura Y, Yanai K, Sekine Y, Uchida Y, Ito S, Terasaki T. Quantitative atlas of membrane transporter proteins: development and application of a highly sensitive simultaneous LC/MS/MS method combined with novel in-silico peptide selection criteria. Pharm. Res. 2008; 25(6):1469–1483. [PubMed: 18219561]

[35]. Dauchy S, Dutheil F, Weaver RJ, Chassoux F, Daumas-Duport C, Couraud PO, Scherrmann JM, De Waziers I, Decleves X. ABC transporters, cytochromes P450 and their main transcription factors: expression at the human blood-brain barrier. J. Neurochem. 2008; 107(6):1518–1528. [PubMed: 19094056]

[36]. Ito K, Uchida Y, Ohtsuki S, Aizawa S, Kawakami H, Katsukura Y, Kamiie J, Terasaki T. Quantitative membrane protein expression at the blood-brain barrier of adult and younger cynomolgus monkeys. J. Pharm. Sci. 2011 in press; DOI: 10.1002/jps.22487.

[37]. Matsson P, Pedersen JM, Norinder U, Bergstrom CA, Artursson P. Identification of novel specific and general inhibitors of the three major human ATP-binding cassette transporters P-gp, BCRP and MRP2 among registered drugs. Pharm. Res. 2009; 26(8):1816–1831. [PubMed: 19421845]

[38]. Rabindran SK, Ross DD, Doyle LA, Yang W, Greenberger LM. Fumitremorgin C reverses multidrug resistance in cells transfected with the breast cancer resistance protein. Cancer Res. 2000; 60(1):47–50. [PubMed: 10646850]

[39]. Allen JD, van Loevezijn A, Lakhai JM, van der Valk M, van Tellingen O, Reid G, Schellens JH, Koomen GJ, Schinkel AH. Potent and specific inhibition of the breast cancer resistance protein multidrug transporter in vitro and in mouse intestine by a novel analogue of fumitremorgin C. Mol. Cancer Ther. 2002; 1(6):417–425. [PubMed: 12477054]

[40]. Kühnle M, Egger M, Müller C, Mahringer A, Bernhardt G, Fricker G, Konig B, Buschauer A. Potent and selective inhibitors of breast cancer resistance protein (ABCG2) derived from the p-glycoprotein (ABCB1) modulator tariquidar. J. Med. Chem. 2009; 52(4):1190–1197. [PubMed: 19170519]

[41]. Giri N, Shaik N, Pan G, Terasaki T, Mukai C, Kitagaki S, Miyakoshi N, Elmquist WF. Investigation of the role of breast cancer resistance protein (Bcrp/Abcg2) on pharmacokinetics and central nervous system penetration of abacavir and zidovudine in the mouse. Drug Metab. Dispos. 2008; 36(8):1476–1484. [PubMed: 18443033]

[42]. Cole SP, Bhardwaj G, Gerlach JH, Mackie JE, Grant CE, Almquist KC, Stewart AJ, Kurz EU, Duncan AM, Deeley RG. Overexpression of a transporter gene in a multidrug-resistant human lung cancer cell line. Science. 1992; 258(5088):1650–1654. [PubMed: 1360704]

[43]. Borst P, Evers R, Kool M, Wijnholds J. A family of drug transporters: the multidrug resistance-associated proteins. J. Natl. Cancer Inst. 2000; 92(16):1295–1302. [PubMed: 10944550]

[44]. Sugiyama D, Kusuhara H, Lee YJ, Sugiyama Y. Involvement of multidrug resistance associated protein 1 (Mrp1) in the efflux transport of 17beta estradiol-D-17beta-glucuronide (E217betaG) across the blood-brain barrier. Pharm. Res. 2003; 20(9):1394–1400. [PubMed: 14567633]

[45]. Cisternino S, Rousselle C, Lorico A, Rappa G, Scherrmann JM. Apparent lack of Mrp1-mediated efflux at the luminal side of mouse blood-brain barrier endothelial cells. Pharm. Res. 2003; 20(6):904–909. [PubMed: 12817896]

[46]. Cattelotte J, Tournier N, Rizzo-Padoin N, Schinkel AH, Scherrmann JM, Cisternino S. Changes in dipole membrane potential at the mouse blood-brain barrier enhance the transport of 99mTechnetium Sestamibi more than inhibiting Abcb1, Abcc1, or Abcg2. J. Neurochem. 2009; 108(3):767–775. [PubMed: 19067785]

[47]. Wijnholds J, deLange EC, Scheffer GL, van den Berg DJ, Mol CA, van der Valk M, Schinkel AH, Scheper RJ, Breimer DD, Borst P. Multidrug resistance protein 1 protects the choroid plexus epithelium and contributes to the blood-cerebrospinal fluid barrier. J. Clin. Invest. 2000; 105(3): 279–285. [PubMed: 10675353]

[48]. Sun H, Johnson DR, Finch RA, Sartorelli AC, Miller DW, Elmquist WF. Transport of fluorescein in MDCKII-MRP1 transfected cells and mrp1-knockout mice. Biochem. Biophys. Res. Commun. 2001; 284(4):863–869. [PubMed: 11409873]

[49]. Sun H, Miller DW, Elmquist WF. Effect of probenecid on fluorescein transport in the central nervous system using in vitro and in vivo models. Pharm. Res. 2001; 18(11):1542–1549. [PubMed: 11758761]

[50]. van Vliet EA, Redeker S, Aronica E, Edelbroek PM, Gorter JA. Expression of multidrug transporters MRP1, MRP2, and BCRP shortly after status epilepticus, during the latent period, and in chronic epileptic rats. Epilepsia. 2005; 46(10):1569–1580. [PubMed: 16190927]

[51]. Innis RB, Cunningham VJ, Delforge J, Fujita M, Gjedde A, Gunn RN, Holden J, Houle S, Huang SC, Ichise M, Iida H, Ito H, Kimura Y, Koeppe RA, Knudsen GM, Knuuti J, Lammertsma AA, Laruelle M, Logan J, Maguire RP, Mintun MA, Morris ED, Parsey R, Price JC, Slifstein M, Sossi V, Suhara T, Votaw JR, Wong DF, Carson RE. Consensus nomenclature for in vivo imaging of reversibly binding radioligands. J. Cereb. Blood Flow Metab. 2007; 27(9):1533–1539. [PubMed: 17519979]

[52]. Hendrikse NH, Schinkel AH, de Vries EG, Fluks E, Van der Graaf WT, Willemsen AT, Vaalburg W, Franssen EJ. Complete in vivo reversal of P-glycoprotein pump function in the blood-brain barrier visualized with positron emission tomography. Br. J. Pharmacol. 1998; 124(7):1413–1418. [PubMed: 9723952]

[53]. Germann UA, Ford PJ, Shlyakhter D, Mason VS, Harding MW. Chemosensitization and drug accumulation effects of VX-710, verapamil, cyclosporin A, MS-209 and GF120918 in multidrug resistant HL60/ADR cells expressing the multidrug resistance-associated protein MRP. Anticancer. Drugs. 1997; 8(2):141–155. [PubMed: 9073310]

[54]. Elsinga PH, Franssen EJ, Hendrikse NH, Fluks L, Weemaes AM, van der Graaf WT, de Vries EG, Visser GM, Vaalburg W. Carbon-11-labeled daunorubicin and verapamil for probing P-glycoprotein in tumors with PET. J. Nucl. Med. 1996; 37(9):1571–1575. [PubMed: 8790221]

[55]. Hendrikse NH, de Vries EG, Eriks-Fluks L, van der Graaf WT, Hospers GA, Willemsen AT, Vaalburg W, Franssen EJ. A new in vivo method to study P-glycoprotein transport in tumors and the blood-brain barrier. Cancer Res. 1999; 59(10):2411–2416. [PubMed: 10344751]

[56]. Bart J, Willemsen AT, Groen HJ, van der Graaf WT, Wegman TD, Vaalburg W, de Vries EG, Hendrikse NH. Quantitative assessment of P-glycoprotein function in the rat blood-brain barrier by distribution volume of [^{11}C]verapamil measured with PET. Neuroimage. 2003; 20(3):1775–1782. [PubMed: 14642487]

[57]. Syvänen S, Blomquist G, Sprycha M, Urban Hoglund A, Roman M, Eriksson O, Hammarlund-Udenaes M, Långström B, Bergström M. Duration and degree of cyclosporin induced P-

glycoprotein inhibition in the rat blood-brain barrier can be studied with PET. Neuroimage. 2006; 32(3):1134–1141. [PubMed: 16857389]

[58]. Kuntner C, Bankstahl JP, Bankstahl M, Stanek J, Wanek T, Stundner G, Karch R, Brauner R, Meier M, Ding XQ, Müller M, Löscher W, Langer O. Dose-response assessment of tariquidar and elacridar and regional quantification of P-glycoprotein inhibition at the rat blood-brain barrier using (*R*)-[^{11}C]verapamil PET. Eur. J. Nucl. Med. Mol. Imaging. 2010; 37(5):942–953. [PubMed: 20016890]

[59]. Wagner CC, Bauer M, Karch R, Feurstein T, Kopp S, Chiba P, Kletter K, Löscher W, Müller M, Zeitlinger M, Langer O. A pilot study to assess the efficacy of tariquidar to inhibit P-glycoprotein at the human blood-brain barrier with (R)-^{11}C-verapamil and PET. J. Nucl. Med. 2009; 50(12): 1954–1961. [PubMed: 19910428]

[60]. Wegman TD, Maas B, Elsinga PH, Vaalburg W. An improved method for the preparation of [^{11}C]verapamil. Appl. Radiat. Isot. 2002; 57(4):505–507. [PubMed: 12361330]

[61]. Hendrikse NH, de Vries EGE, Franssen EJF, Vaalburg W, van der Graaf WTA. In vivo measurement of [^{11}C]verapamil kinetics in human tissues. Eur. J. Clin. Pharmacol. 2001; 56:827–829. [PubMed: 11294373]

[62]. Sasongko L, Link JM, Muzi M, Mankoff DA, Yang X, Collier AC, Shoner SC, Unadkat JD. Imaging P-glycoprotein transport activity at the human blood-brain barrier with positron emission tomography. Clin. Pharmacol. Ther. 2005; 77(6):503–514. [PubMed: 15961982]

[63]. Muzi M, Mankoff DA, Link JM, Shoner S, Collier AC, Sasongko L, Unadkat JD. Imaging of Cyclosporine Inhibition of P-Glycoprotein Activity Using ^{11}C-Verapamil in the Brain: Studies of Healthy Humans. J. Nucl. Med. 2009; 50(8):1267–1275. [PubMed: 19617341]

[64]. Ikoma Y, Takano A, Ito H, Kusuhara H, Sugiyama Y, Arakawa R, Fukumura T, Nakao R, Suzuki K, Suhara T. Quantitative analysis of ^{11}C-verapamil transfer at the human blood-brain barrier for evaluation of P-glycoprotein function. J. Nucl. Med. 2006; 47(9):1531–1537. [PubMed: 16954563]

[65]. Lee YJ, Maeda J, Kusuhara H, Okauchi T, Inaji M, Nagai Y, Obayashi S, Nakao R, Suzuki K, Sugiyama Y, Suhara T. In vivo evaluation of P-glycoprotein function at the blood-brain barrier in nonhuman primates using [^{11}C]verapamil. J. Pharmacol. Exp. Ther. 2006; 316(2):647–653. [PubMed: 16293715]

[66]. Chung FS, Eyal S, Muzi M, Link JM, Mankoff DA, Kaddoumi A, O'Sullivan F, Hsiao P, Unadkat JD. Positron emission tomography imaging of tissue P-glycoprotein activity during pregnancy in the non-human primate. Br. J. Pharmacol. 2010; 159(2):394–404. [PubMed: 20002098]

[67]. Eyal S, Chung FS, Muzi M, Link JM, Mankoff DA, Kaddoumi A, O'Sullivan F, Hebert MF, Unadkat JD. Simultaneous PET imaging of P-glycoprotein inhibition in multiple tissues in the pregnant nonhuman primate. J. Nucl. Med. 2009; 50(5):798–806. [PubMed: 19403878]

[68]. Brunner M, Langer O, Sunder-Plassmann R, Dobrozemsky G, Müller U, Wadsak W, Krcal A, Karch R, Mannhalter C, Dudczak R, Kletter K, Steiner I, Baumgartner C, Müller M. Influence of functional haplotypes in the drug transporter gene ABCB1 on central nervous system drug distribution in humans. Clin. Pharmacol. Ther. 2005; 78(2):182–190. [PubMed: 16084852]

[69]. Takano A, Kusuhara H, Suhara T, Ieiri I, Morimoto T, Lee YJ, Maeda J, Ikoma Y, Ito H, Suzuki K, Sugiyama Y. Evaluation of in vivo P-glycoprotein function at the blood-brain barrier among MDR1 gene polymorphisms by using ^{11}C-verapamil. J. Nucl. Med. 2006; 47(9):1427–1433. [PubMed: 16954549]

[70]. Luurtsema G, Windhorst AD, Mooijer MPJ, Herscheid JDM, Lammertsma AA, Franssen EJF. Fully automated high yield synthesis of (R)- and (S)-[C-11]verapamil for measuring P-glycoprotein function with positron emission tomography. J. Labelled Cpd. Radiopharm. 2002; 45(14):1199–1207.

[71]. Luurtsema G, Molthoff CF, Windhorst AD, Smit JW, Keizer H, Boellaard R, Lammertsma AA, Franssen EJ. (R)- and (S)-[^{11}C]verapamil as PET-tracers for measuring P-glycoprotein function: in vitro and in vivo evaluation. Nucl. Med. Biol. 2003; 30(7):747–751. [PubMed: 14499333]

[72]. Eichelbaum M, Mikus G, Vogelgesang B. Pharmacokinetics of (+)-, (−)- and (+/−)-verapamil after intravenous administration. Br. J. Clin. Pharmacol. 1984; 17(4):453–458. [PubMed: 6721991]

[73]. Luurtsema G, Molthoff CF, Schuit RC, Windhorst AD, Lammertsma AA, Franssen EJ. Evaluation of (*R*)-[^{11}C]verapamil as PET tracer of P-glycoprotein function in the blood-brain barrier: kinetics and metabolism in the rat. Nucl. Med. Biol. 2005; 32(1):87–93. [PubMed: 15691665]

[74]. Lubberink M, Luurtsema G, van Berckel BN, Boellaard R, Toornvliet R, Windhorst AD, Franssen EJ, Lammertsma AA. Evaluation of tracer kinetic models for quantification of P-glycoprotein function using (R)-[(11)C]verapamil and PET. J. Cereb. Blood Flow Metab. 2007; 27(2):424–433. [PubMed: 16757979]

[75]. Pauli-Magnus C, von Richter O, Burk O, Ziegler A, Mettang T, Eichelbaum M, Fromm MF. Characterization of the major metabolites of verapamil as substrates and inhibitors of P-glycoprotein. J. Pharmacol. Exp. Ther. 2000; 293(2):376–382. [PubMed: 10773005]

[76]. Abrahim A, Luurtsema G, Bauer M, Karch R, Lubberink M, Pataraia E, Joukhadar C, Kletter K, Lammertsma AA, Baumgartner C, Müller M, Langer O. Peripheral metabolism of (R)-[(11)C]verapamil in epilepsy patients. Eur. J. Nucl. Med. Mol. Imaging. 2008; 35:116–123. [PubMed: 17846766]

[77]. Bankstahl JP, Kuntner C, Abrahim A, Karch R, Stanek J, Wanek T, Wadsak W, Kletter K, Müller M, Löscher W, Langer O. Tariquidar-induced P-glycoprotein inhibition at the rat blood-brain barrier studied with (R)-^{11}C-verapamil and PET. J. Nucl. Med. 2008; 49(8):1328–1335. [PubMed: 18632828]

[78]. Bankstahl JP, Löscher W. Resistance to antiepileptic drugs and expression of P-glycoprotein in two rat models of status epilepticus. Epilepsy Res. 2008; 82(1):70–85. [PubMed: 18760905]

[79]. Syvänen S, Luurtsema G, Molthoff CF, Windhorst AD, Huisman MC, Lammertsma AA, Voskuyl RA, de Lange EC. (R)-[^{11}C]Verapamil PET studies to assess changes in P-glycoprotein expression and functionality in rat blood-brain barrier after exposure to kainate-induced status epilepticus. BMC Med. Imaging. 2011; 11:1–16. [PubMed: 21199574]

[80]. Bauer M, Karch R, Neumann F, Wagner CC, Kletter K, Müller M, Löscher W, Zeitlinger M, Langer O. Assessment of regional differences in tariquidar-induced P-glycoprotein modulation at the human blood-brain barrier. J. Cereb. Blood Flow Metab. 2010; 30(3):510–515. [PubMed: 20010957]

[81]. Eyal S, Ke B, Muzi M, Link JM, Mankoff DA, Collier AC, Unadkat JD. Regional P-Glycoprotein Activity and Inhibition at the Human Blood-Brain Barrier as Imaged by Positron Emission Tomography. Clin. Pharmacol. Ther. 2010; 87(5):579–585. [PubMed: 20336065]

[82]. Kreisl WC, Liow JS, Kimura N, Seneca N, Zoghbi SS, Morse CL, Herscovitch P, Pike VW, Innis RB. P-glycoprotein function at the blood-brain barrier in humans can be quantified with the substrate radiotracer ^{11}C-N-desmethyl-loperamide. J. Nucl. Med. 2010; 51(4):559–566. [PubMed: 20237038]

[83]. Bartels AL, Kortekaas R, Bart J, Willemsen AT, de Klerk OL, de Vries JJ, van Oostrom JC, Leenders KL. Blood-brain barrier P-glycoprotein function decreases in specific brain regions with aging: A possible role in progressive neurodegeneration. Neurobiol. Aging. 2009; 30(11): 1818–1824. [PubMed: 18358568]

[84]. Bauer M, Karch R, Neumann F, Abrahim A, Wagner CC, Kletter K, Müller M, Zeitlinger M, Langer O. Age dependency of cerebral P-gp function measured with (*R*)-[^{11}C]verapamil and PET. Eur. J. Clin. Pharmacol. 2009; 65(9):941–946. [PubMed: 19655132]

[85]. Toornvliet R, van Berckel BN, Luurtsema G, Lubberink M, Geldof AA, Bosch TM, Oerlemans R, Lammertsma AA, Franssen EJ. Effect of age on functional P-glycoprotein in the blood-brain barrier measured by use of (R)-[(11)C]verapamil and positron emission tomography. Clin. Pharmacol. Ther. 2006; 79(6):540–548. [PubMed: 16765142]

[86]. Langer O, Bauer M, Hammers A, Karch R, Pataraia E, Koepp MJ, Abrahim A, Luurtsema G, Brunner M, Sunder-Plassmann R, Zimprich F, Joukhadar C, Gentzsch S, Dudczak R, Kletter K, Müller M, Baumgartner C. Pharmacoresistance in epilepsy: a pilot PET study with the P-glycoprotein substrate R-[^{11}C]verapamil. Epilepsia. 2007; 48(9):1774–1784. [PubMed: 17484754]

[87]. Bartels AL, Willemsen AT, Kortekaas R, de Jong BM, de Vries R, de Klerk O, van Oostrom JC, Portman A, Leenders KL. Decreased blood-brain barrier P-glycoprotein function in the

progression of Parkinson's disease, PSP and MSA. J. Neural Transm. 2008; 115(7):1001–1009. [PubMed: 18265929]

[88]. de Klerk OL, Willemsen AT, Roosink M, Bartels AL, Harry Hendrikse N, Bosker FJ, den Boer JA. Locally increased P-glycoprotein function in major depression: a PET study with [^{11}C]verapamil as a probe for P-glycoprotein function in the blood-brain barrier. Int. J. Neuropsychopharmacol. 2009; 12:895–904. [PubMed: 19224656]

[89]. Kortekaas R, Leenders KL, van Oostrom JC, Vaalburg W, Bart J, Willemsen AT, Hendrikse NH. Blood-brain barrier dysfunction in parkinsonian midbrain in vivo. Ann. Neurol. 2005; 57(2):176–179. [PubMed: 15668963]

[90]. de Klerk OL, Willemsen AT, Bosker FJ, Bartels AL, Hendrikse NH, den Boer JA, Dierckx RA. Regional increase in P-glycoprotein function in the blood-brain barrier of patients with chronic schizophrenia: a PET study with [(11)C]verapamil as a probe for P-glycoprotein function. Psychiatry Res. 2010; 183(2):151–156. [PubMed: 20620031]

[91]. Zoghbi SS, Liow JS, Yasuno F, Hong J, Tuan E, Lazarova N, Gladding RL, Pike VW, Innis RB. ^{11}C-loperamide and its N-desmethyl radiometabolite are avid substrates for brain permeability-glycoprotein efflux. J. Nucl. Med. 2008; 49(4):649–656. [PubMed: 18344435]

[92]. Kannan P, Brimacombe KR, Zoghbi SS, Liow JS, Morse C, Taku AK, Pike VW, Halldin C, Innis RB, Gottesman MM, Hall MD. N-desmethyl-loperamide is selective for P-glycoprotein among three ATP-binding cassette transporters at the blood-brain barrier. Drug Metab. Dispos. 2010; 38(6):917–922. [PubMed: 20212014]

[93]. Lazarova N, Zoghbi SS, Hong J, Seneca N, Tuan E, Gladding RL, Liow JS, Taku A, Innis RB, Pike VW. Synthesis and evaluation of [N-methyl-^{11}C]N-desmethyl-loperamide as a new and improved PET radiotracer for imaging P-gp function. J. Med. Chem. 2008; 51(19):6034–6043. [PubMed: 18783208]

[94]. Liow JS, Kreisl W, Zoghbi SS, Lazarova N, Seneca N, Gladding RL, Taku A, Herscovitch P, Pike VW, Innis RB. P-Glycoprotein Function at the Blood-Brain Barrier Imaged Using ^{11}C-N-Desmethyl-Loperamide in Monkeys. J. Nucl. Med. 2009; 50(1):108–115. [PubMed: 19091890]

[95]. Kannan P, Brimacombe KR, Kreisl WC, Liow JS, Zoghbi SS, Telu S, Zhang Y, Pike VW, Halldin C, Gottesman MM, Innis RB, Hall MD. Lysosomal trapping of a radiolabeled substrate of P-glycoprotein as a mechanism for signal amplification in PET. Proc. Natl. Acad. Sci. U. S. A. 2011; 108(6):2593–2598. [PubMed: 21262843]

[96]. Seneca N, Zoghbi SS, Shetty HU, Tuan E, Kannan P, Taku A, Innis RB, Pike VW. Effects of ketoconazole on the biodistribution and metabolism of [^{11}C]loperamide and [^{11}C]N-desmethyl-loperamide in wild-type and P-gp knockout mice. Nucl. Med. Biol. 2010; 37(3):335–345. [PubMed: 20346873]

[97]. Doze P, Elsinga PH, Maas B, Van Waarde A, Wegman T, Vaalburg W. Synthesis and evaluation of radiolabeled antagonists for imaging of beta-adrenoceptors in the brain with PET. Neurochem. Int. 2002; 40(2):145–155. [PubMed: 11738481]

[98]. Jonsson O, Behnam-Motlagh P, Persson M, Henriksson R, Grankvist K. Increase in doxorubicin cytotoxicity by carvedilol inhibition of P-glycoprotein activity. Biochem. Pharmacol. 1999; 58(11):1801–1806. [PubMed: 10571255]

[99]. Bart J, Dijkers EC, Wegman TD, de Vries EG, van der Graaf WT, Groen HJ, Vaalburg W, Willemsen AT, Hendrikse NH. New positron emission tomography tracer [(11)C]carvedilol reveals P-glycoprotein modulation kinetics. Br. J. Pharmacol. 2005; 145(8):1045–1051. [PubMed: 15951832]

[100]. Levchenko A, Mehta BM, Lee JB, Humm JL, Augensen F, Squire O, Kothari PJ, Finn RD, Leonard EF, Larson SM. Evaluation of ^{11}C-colchicine for PET imaging of multiple drug resistance. J. Nucl. Med. 2000; 41(3):493–501. [PubMed: 10716325]

[101]. van Tilburg E, Franssen E, van der Hoeven J, van der Meij M, Elshove D, Lammertsma A, Windhorst A. Radiosynthesis of [C-11]docetaxel. J. Labelled Cpd. Radiopharm. 2004; 47(11): 763–777.

[102]. van Tilburg EW, Mooijer MPJ, Brinkhorst J, van der Meij M, Windhorst AD. Improved and semi-automated GMP-compliant radiosynthesis of [^{11}C]docetaxel. Appl. Radiat. Isot. 2008; 66(10):1414–1418. [PubMed: 18394910]

[103]. van der Veldt AA, Hendrikse NH, Smit EF, Mooijer MP, Rijnders AY, Gerritsen WR, van der Hoeven JJ, Windhorst AD, Lammertsma AA, Lubberink M. Biodistribution and radiation dosimetry of ^{11}C-labelled docetaxel in cancer patients. Eur. J. Nucl. Med. Mol. Imaging. 2010; 37(10):1950–1958. [PubMed: 20508935]

[104]. Kawamura K, Yamasaki T, Yui J, Hatori A, Konno F, Kumata K, Irie T, Fukumura T, Suzuki K, Kanno I, Zhang MR. In vivo evaluation of P-glycoprotein and breast cancer resistance protein modulation in the brain using [(11)C]gefitinib. Nucl. Med. Biol. 2009; 36(3):239–246. [PubMed: 19324269]

[105]. Wang JQ, Gao M, Miller KD, Sledge GW, Zheng QH. Synthesis of [^{11}C]Iressa as a new potential PET cancer imaging agent for epidermal growth factor receptor tyrosine kinase. Bioorg. Med. Chem. Lett. 2006; 16(15):4102–4106. [PubMed: 16697188]

[106]. Passchier J, van Waarde A, Doze P, Elsinga PH, Vaalburg W. Influence of P-glycoprotein on brain uptake of [^{18}F]MPPF in rats. Eur. J. Pharmacol. 2000; 407(3):273–280. [PubMed: 11068023]

[107]. Laćan G, Plenevaux A, Rubins DJ, Way BM, Defraiteur C, Lemaire C, Aerts J, Luxen A, Cherry SR, Melega WP. Cyclosporine, a P-glycoprotein modulator, increases [^{18}F]MPPF uptake in rat brain and peripheral tissues: microPET and ex vivo studies. Eur. J. Nucl. Med. Mol. Imaging. 2008; 35(12):2256–2266. [PubMed: 18604533]

[108]. la Fougere C, Boning G, Bartmann H, Wangler B, Nowak S, Just T, Wagner E, Winter P, Rominger A, Forster S, Gildehaus FJ, Rosa-Neto P, Minuzzi L, Bartenstein P, Potschka H, Cumming P. Uptake and binding of the serotonin 5-HT(1A) antagonist [(18)F]-MPPF in brain of rats: Effects of the novel P-glycoprotein inhibitor tariquidar. Neuroimage. 2010; 49(2):1406–1415. [PubMed: 19796699]

[109]. Bartmann H, Fuest C, la Fougere C, Xiong G, Just T, Schlichtiger J, Winter P, Boning G, Wangler B, Pekcec A, Soerensen J, Bartenstein P, Cumming P, Potschka H. Imaging of P-glycoprotein-mediated pharmacoresistance in the hippocampus: proof-of-concept in a chronic rat model of temporal lobe epilepsy. Epilepsia. 2010; 51(9):1780–1790. [PubMed: 20633036]

[110]. Merlet I, Ostrowsky K, Costes N, Ryvlin P, Isnard J, Faillenot I, Lavenne F, Dufournel D, Le Bars D, Mauguiere F. 5-HT1A receptor binding and intracerebral activity in temporal lobe epilepsy: an [^{18}F]MPPF-PET study. Brain. 2004; 127(Pt 4):900–913. [PubMed: 14985263]

[111]. Schinkel AH, Mayer U, Wagenaar E, Mol CA, van Deemter L, Smit JJ, van der Valk MA, Voordouw AC, Spits H, van Tellingen O, Zijlmans JM, Fibbe WE, Borst P. Normal viability and altered pharmacokinetics in mice lacking mdr1-type (drug-transporting) P-glycoproteins. Proc. Natl. Acad. Sci. U. S. A. 1997; 94(8):4028–4033. [PubMed: 9108099]

[112]. McGrogan BT, Gilmartin B, Carney DN, McCann A. Taxanes, microtubules and chemoresistant breast cancer. Biochim. Biophys. Acta. 2008; 1785(2):96–132. [PubMed: 18068131]

[113]. Ravert HT, Klecker RW, Collins JM, Mathews WB, Pomper MG, Wahl RL, Dannals RF. Radiosynthesis of [C-11]paclitaxel. J. Labelled Cpd. Radiopharm. 2002; 45(6):471–477.

[114]. Roh EJ, Park YH, Song CE, Oh SJ, Choe YS, Kim BT, Chi DY, Kim D. Radiolabeling of paclitaxel with electrophilic 123I. Bioorg. Med. Chem. 2000; 8(1):65–68. [PubMed: 10968265]

[115]. Kiesewetter DO, Jagoda EM, Kao CH, Ma Y, Ravasi L, Shimoji K, Szajek LP, Eckelman WC. Fluoro-, bromo-, and iodopaclitaxel derivatives: synthesis and biological evaluation. Nucl. Med. Biol. 2003; 30(1):11–24. [PubMed: 12493538]

[116]. Li C, Yu DF, Inoue T, Yang DJ, Tansey W, Liu CW, Milas L, Hunter NR, Kim EE, Wallace S. Synthesis, biodistribution and imaging properties of indium-111-DTPA-paclitaxel in mice bearing mammary tumors. J. Nucl. Med. 1997; 38(7):1042–1047. [PubMed: 9225788]

[117]. Kalen JD, Hirsch JI, Kurdziel KA, Eckelman WC, Kiesewetter DO. Automated synthesis of ^{18}F analogue of paclitaxel (PAC): [^{18}F]Paclitaxel (FPAC). Appl. Radiat. Isot. 2007; 65(6):696–700. [PubMed: 17161952]

[118]. Kurdziel KA, Kiesewetter DO, Carson RE, Eckelman WC, Herscovitch P. Biodistribution, radiation dose estimates, and in vivo Pgp modulation studies of ^{18}F-paclitaxel in nonhuman primates. J. Nucl. Med. 2003; 44(8):1330–1339. [PubMed: 12902425]

[119]. Gangloff A, Hsueh WA, Kesner AL, Kiesewetter DO, Pio BS, Pegram MD, Beryt M, Townsend A, Czernin J, Phelps ME, Silverman DH. Estimation of paclitaxel biodistribution and

uptake in human-derived xenografts in vivo with (18)F-fluoropaclitaxel. J. Nucl. Med. 2005; 46(11):1866–1871. [PubMed: 16269601]

[120]. Hsueh WA, Kesner AL, Gangloff A, Pegram MD, Beryt M, Czernin J, Phelps ME, Silverman DH. Predicting chemotherapy response to paclitaxel with ^{18}F-Fluoropaclitaxel and PET. J. Nucl. Med. 2006; 47(12):1995–1999. [PubMed: 17138742]

[121]. Luna-Tortos C, Fedrowitz M, Löscher W. Several major antiepileptic drugs are substrates for human P-glycoprotein. Neuropharmacology. 2008; 55(8):1364–1375. [PubMed: 18824002]

[122]. Potschka H, Löscher W. In vivo evidence for P-glycoprotein-mediated transport of phenytoin at the blood-brain barrier of rats. Epilepsia. 2001; 42(10):1231–1240. [PubMed: 11737157]

[123]. van Vliet EA, van Schaik R, Edelbroek PM, Redeker S, Aronica E, Wadman WJ, Marchi N, Vezzani A, Gorter JA. Inhibition of the multidrug transporter P-glycoprotein improves seizure control in phenytoin-treated chronic epileptic rats. Epilepsia. 2006; 47(4):672–680. [PubMed: 16650133]

[124]. Potschka H, Fedrowitz M, Löscher W. Multidrug resistance protein MRP2 contributes to blood-brain barrier function and restricts antiepileptic drug activity. J. Pharmacol. Exp. Ther. 2003; 306(1):124–131. [PubMed: 12663688]

[125]. Stavchansky SA, Tilbury RS, McDonald JM, Ting CT, Kostenbauder HB. In vivo distribution of carbon-11 phenytoin and its major metabolite, and their use in scintigraphic imaging. J. Nucl. Med. 1978; 19(8):936–941. [PubMed: 98619]

[126]. Roeda D, Westera G. The Synthesis of Some C-11-Labeled Anti-Epileptic Drugs with Potential Utility as Radiopharmaceuticals - Hydantoins and Barbiturates. Int. J. Appl. Radiat. Isot. 1981; 32(11):843–845. [PubMed: 7309275]

[127]. Baron JC, Roeda D, Munari C, Crouzel C, Chodkiewicz JP, Comar D. Brain regional pharmacokinetics of ^{11}C-labeled diphenylhydantoin: positron emission tomography in humans. Neurology. 1983; 33(5):580–585. [PubMed: 6601779]

[128]. Piwnica-Worms D, Kesarwala AH, Pichler A, Prior JL, Sharma V. Single photon emission computed tomography and positron emission tomography imaging of multi-drug resistant P-glycoprotein--monitoring a transport activity important in cancer, blood-brain barrier function and Alzheimer's disease. Neuroimaging Clin. N. Am. 2006; 16(4):575–589. viii. [PubMed: 17148020]

[129]. Marian T, Szabo G, Goda K, Nagy H, Szincsak N, Juhasz I, Galuska L, Balkay L, Mikecz P, Tron L, Krasznai Z. In vivo and in vitro multitracer analyses of P-glycoprotein expression-related multidrug resistance. Eur. J. Nucl. Med. Mol. Imaging. 2003; 30(8):1147–1154. [PubMed: 12830325]

[130]. van Leeuwen FW, Buckle T, Kersbergen A, Rottenberg S, Gilhuijs KG. Noninvasive functional imaging of P-glycoprotein-mediated doxorubicin resistance in a mouse model of hereditary breast cancer to predict response, and assign P-gp inhibitor sensitivity. Eur. J. Nucl. Med. Mol. Imaging. 2009; 36(3):406–412. [PubMed: 19093112]

[131]. Wang JH, Scollard DA, Teng S, Reilly RM, Piquette-Miller M. Detection of P-glycoprotein activity in endotoxemic rats by ^{99m}Tc-sestamibi imaging. J. Nucl. Med. 2005; 46(9):1537–1545. [PubMed: 16157538]

[132]. Gomes CM, Abrunhosa AJ, Pauwels EK, Botelho MF. P-glycoprotein versus MRP1 on transport kinetics of cationic lipophilic substrates: a comparative study using [^{99m}Tc]sestamibi and [^{99m}Tc]tetrofosmin. Cancer Biother. Radiopharm. 2009; 24(2):215–227. [PubMed: 19409044]

[133]. Abraham J, Edgerly M, Wilson R, Chen C, Rutt A, Bakke S, Robey R, Dwyer A, Goldspiel B, Balis F, Van Tellingen O, Bates SE, Fojo T. A phase I study of the P-glycoprotein antagonist tariquidar in combination with vinorelbine. Clin. Cancer Res. 2009; 15(10):3574–3782. [PubMed: 19417029]

[134]. Agrawal M, Abraham J, Balis FM, Edgerly M, Stein WD, Bates S, Fojo T, Chen CC. Increased ^{99m}Tc-sestamibi accumulation in normal liver and drug-resistant tumors after the administration of the glycoprotein inhibitor, XR9576. Clin. Cancer Res. 2003; 9(2):650–656. [PubMed: 12576431]

[135]. Kelly RJ, Draper D, Chen CC, Robey RW, Figg WD, Piekarz RL, Chen X, Gardner ER, Balis FM, Venkatesan AM, Steinberg SM, Fojo AT, Bates SE. A Pharmacodynamic Study of Docetaxel in Combination with the P-glycoprotein Antagonist, Tariquidar (XR9576) in Patients with Lung, Ovarian, and Cervical Cancer. Clin. Cancer Res. 2011; 17(3):569–580. [PubMed: 21081657]

[136]. Bigott HM, Prior JL, Piwnica-Worms DR, Welch MJ. Imaging multidrug resistance P-glycoprotein transport function using microPET with technetium-94m-sestamibi. Mol. Imaging. 2005; 4(1):30–39. [PubMed: 15967124]

[137]. Chen WS, Luker KE, Dahlheimer JL, Pica CM, Luker GD, Piwnica-Worms D. Effects of MDR1 and MDR3 P-glycoproteins, MRP1, and BCRP/MXR/ABCP on the transport of (99m)Tc-tetrofosmin. Biochem. Pharmacol. 2000; 60(3):413–426. [PubMed: 10856437]

[138]. van Waarde A, Ramakrishnan NK, Rybczynska AA, Elsinga PH, Berardi F, de Jong JR, Kwizera C, Perrone R, Cantore M, Sijbesma JWA, Dierckx RA, Colabufo NA. Synthesis and preclinical evaluation of novel PET probes for p-glycoprotein function and expression. J. Med. Chem. 2009; 52(14):4524–4532. [PubMed: 19530699]

[139]. Bruyne SD, Wyffels L, Moerman L, Sambre J, Colabufo NA, Berardi F, Perrone R, Vos FD. Radiosynthesis and in vivo evaluation of [(11)C]MC80 for P-glycoprotein imaging. Bioorg. Med. Chem. 2010; 18(17):6489–6495. [PubMed: 20685124]

[140]. Ishiwata K, Kawamura K, Yanai K, Hendrikse NH. In vivo evaluation of P-glycoprotein modulation of 8 PET radioligands used clinically. J. Nucl. Med. 2007; 48(1):81–87. [PubMed: 17204702]

[141]. Doze P, Van Waarde A, Elsinga PH, Hendrikse NH, Vaalburg W. Enhanced cerebral uptake of receptor ligands by modulation of P-glycoprotein function in the blood-brain barrier. Synapse. 2000; 36(1):66–74. [PubMed: 10700027]

[142]. Vries EF, Kortekaas R, van Waarde A, Dijkstra D, Elsinga PH, Vaalburg W. Synthesis and evaluation of dopamine D3 receptor antagonist ^{11}C-GR218231 as PET tracer for P-glycoprotein. J. Nucl. Med. 2005; 46(8):1384–1392. [PubMed: 16085598]

[143]. Liow JS, Lu S, McCarron JA, Hong J, Musachio JL, Pike VW, Innis RB, Zoghbi SS. Effect of a P-glycoprotein inhibitor, Cyclosporin A, on the disposition in rodent brain and blood of the 5-HT1A receptor radioligand, [^{11}C](R)-(-)-RWAY. Synapse. 2007; 61(2):96–105. [PubMed: 17117422]

[144]. De Bruyne S, Wyffels L, Boos TL, Staelens S, Deleye S, Rice KC, De Vos F. In vivo evaluation of [^{123}I]-4-(2-(bis(4-fluorophenyl)methoxy)ethyl)-1-(4-iodobenzyl)piperidine, an iodinated SPECT tracer for imaging the P-gp transporter. Nucl. Med. Biol. 2010; 37(4):469–477. [PubMed: 20447559]

[145]. Wong DF, Yung B, Dannals RF, Shaya EK, Ravert HT, Chen CA, Chan B, Folio T, Scheffel U, Ricaurte GA. In vivo imaging of baboon and human dopamine transporters by positron emission tomography using [^{11}C]WIN 35,428. Synapse. 1993; 15(2):130–142. [PubMed: 8259524]

[146]. Ginovart N, Wilson AA, Meyer JH, Hussey D, Houle S. Positron emission tomography quantification of [^{11}C]-DASB binding to the human serotonin transporter: modeling strategies. J. Cereb. Blood Flow Metab. 2001; 21(11):1342–1353. [PubMed: 11702049]

[147]. Luurtsema G, Schuit RC, Klok RP, Verbeek J, Leysen JE, Lammertsma AA, Windhorst AD. Evaluation of [^{11}C]laniquidar as a tracer of P-glycoprotein: radiosynthesis and biodistribution in rats. Nucl. Med. Biol. 2009; 36(6):643–649. [PubMed: 19647170]

[148]. Dörner B, Kuntner C, Bankstahl JP, Bankstahl M, Stanek J, Wanek T, Stundner G, Mairinger S, Löscher W, Müller M, Langer O, Erker T. Synthesis and small-animal positron emission tomography evaluation of [^{11}C]-elacridar as a radiotracer to assess the distribution of P-glycoprotein at the blood-brain barrier. J. Med. Chem. 2009; 52(19):6073–6082. [PubMed: 19711894]

[149]. Kawamura K, Yamasaki T, Konno F, Yui J, Hatori A, Yanamoto K, Wakizaka H, Takei M, Kimura Y, Fukumura T, Zhang MR. Evaluation of Limiting Brain Penetration Related to P-glycoprotein and Breast Cancer Resistance Protein Using [(11)C]GF120918 by PET in Mice. Mol. Imaging Biol. 2011; 13(1):152–160. [PubMed: 20379788]

[150]. Bauer F, Kuntner C, Bankstahl JP, Wanek T, Bankstahl M, Stanek J, Mairinger S, Dörner B, Löscher W, Müller M, Erker T, Langer O. Synthesis and in vivo evaluation of [^{11}C]tariquidar, a

positron emission tomography radiotracer based on a third-generation P-glycoprotein inhibitor. Bioorg. Med. Chem. 2010; 18(15):5489–5497. [PubMed: 20621487]

[151]. Kawamura K, Konno F, Yui J, Yamasaki T, Hatori A, Yanamoto K, Wakizaka H, Takei M, Nengaki N, Fukumura T, Zhang MR. Synthesis and evaluation of [(11)C]XR9576 to assess the function of drug efflux transporters using PET. Ann. Nucl. Med. 2010; 24(5):403–412. [PubMed: 20361276]

[152]. Yamasaki T, Kawamura K, Hatori A, Yui J, Yanamoto K, Yoshida Y, Ogawa M, Nengaki N, Wakisaka H, Fukumura T, Zhang MR. PET study on mice bearing human colon adenocarcinoma cells using [^{11}C]GF120918, a dual radioligand for P-glycoprotein and breast cancer resistance protein. Nucl. Med. Commun. 2010; 31(11):985–993. [PubMed: 20859232]

[153]. Kawamura K, Yamasaki T, Konno F, Yui J, Hatori A, Yanamoto K, Wakizaka H, Ogawa M, Yoshida Y, Nengaki N, Fukumura T, Zhang MR. Synthesis and in vivo evaluation of ^{18}F-fluoroethyl GF120918 and XR9576 as positron emission tomography probes for assessing the function of drug efflux transporters. Bioorg. Med. Chem. 2011; 19(2):861–870. [PubMed: 21185730]

[154]. Polli JW, Wring SA, Humphreys JE, Huang L, Morgan JB, Webster LO, Serabjit-Singh CS. Rational use of in vitro P-glycoprotein assays in drug discovery. J. Pharmacol. Exp. Ther. 2001; 299(2):620–628. [PubMed: 11602674]

[155]. Colabufo NA, Berardi F, Cantore M, Perrone MG, Contino M, Inglese C, Niso M, Perrone R, Azzariti A, Simone GM, Porcelli L, Paradiso A. Small P-gp modulating molecules: SAR studies on tetrahydroisoquinoline derivatives. Bioorg. Med. Chem. 2008; 16:362–373. [PubMed: 17936633]

[156]. Martin C, Berridge G, Mistry P, Higgins C, Charlton P, Callaghan R. The molecular interaction of the high affinity reversal agent XR9576 with P-glycoprotein. Br. J. Pharmacol. 1999; 128(2): 403–411. [PubMed: 10510451]

[157]. Martin C, Berridge G, Mistry P, Higgins C, Charlton P, Callaghan R. Drug binding sites on P-glycoprotein are altered by ATP binding prior to nucleotide hydrolysis. Biochemistry (Mosc). 2000; 39(39):11901–11906.

[158]. Rothnie A, Storm J, McMahon R, Taylor A, Kerr ID, Callaghan R. The coupling mechanism of P-glycoprotein involves residue L339 in the sixth membrane spanning segment. FEBS Lett. 2005; 579(18):3984–3990. [PubMed: 16004994]

[159]. Kannan P, Telu S, Shukla S, Ambudkar SV, Pike VW, Halldin C, Gottesman MM, Innis RB, Hall MD. The “specific” P-glycoprotein inhibitor tariquidar is also a substrate and an inhibitor for breast cancer resistance protein (BCRP/ABCG2). ACS Chem. Neurosci. 2010; 2(2):82–89. [PubMed: 22778859]

[160]. Xia CQ, Liu N, Miwa GT, Gan LS. Interactions of cyclosporin a with breast cancer resistance protein. Drug Metab. Dispos. 2007; 35(4):576–582. [PubMed: 17220244]

[161]. Muenster U, Grieshop B, Ickenroth K, Gnoth MJ. Characterization of substrates and inhibitors for the in vitro assessment of Bcrp mediated drug-drug interactions. Pharm. Res. 2008; 25(10): 2320–2326. [PubMed: 18523872]

[162]. Eckelman WC, Mathis CA. Targeting proteins in vivo: in vitro guidelines. Nucl. Med. Biol. 2006; 33(2):161–164. [PubMed: 16546669]

[163]. Enokizono J, Kusuhara H, Ose A, Schinkel AH, Sugiyama Y. Quantitative investigation of the role of breast cancer resistance protein (Bcrp/Abcg2) in limiting brain and testis penetration of xenobiotic compounds. Drug Metab. Dispos. 2008; 36(6):995–1002. [PubMed: 18322075]

[164]. Kodaira H, Kusuhara H, Ushiki J, Fuse E, Sugiyama Y. Kinetic analysis of the cooperation of P-glycoprotein (P-gp/Abcb1) and breast cancer resistance protein (Bcrp/Abcg2) in limiting the brain and testis penetration of erlotinib, flavopiridol, and mitoxantrone. J. Pharmacol. Exp. Ther. 2010; 333(3):788–796. [PubMed: 20304939]

[165]. Takada Y, Ogawa M, Suzuki H, Fukumura T. Radiosynthesis of [2-(11)C-carbonyl]dantrolene using [(11)C]phosgene for PET. Appl. Radiat. Isot. 2010; 68(9):1715–1720. [PubMed: 20395154]

[166]. Mairinger S, Langer O, Kuntner C, Wanek T, Bankstahl JP, Bankstahl M, Stanek J, Dörner B, Bauer F, Baumgartner C, Löscher W, Erker T, Müller M. Synthesis and in vivo evaluation of the

putative breast cancer resistance protein inhibitor [^{11}C]methyl 4-((4-(2-(6,7-dimethoxy-1,2,3,4-tetrahydroisoquinolin-2-yl)ethyl)phenyl)am ino-carbonyl)-2-(quinoline-2-carbonylamino)benzoate. Nucl. Med. Biol. 2010; 37(5):637–644. [PubMed: 20610168]

[167]. Wang M, Zheng DX, Luo MB, Gao M, Miller KD, Hutchins GD, Zheng QH. Synthesis of carbon-11-labeled tariquidar derivatives as new PET agents for imaging of breast cancer resistance protein (ABCG2). Appl. Radiat. Isot. 2010; 68(6):1098–1103. [PubMed: 20181488]

[168]. de Vries NA, Zhao J, Kroon E, Buckle T, Beijnen JH, van Tellingen O. P-glycoprotein and breast cancer resistance protein: two dominant transporters working together in limiting the brain penetration of topotecan. Clin. Cancer Res. 2007; 13(21):6440–6449. [PubMed: 17975156]

[169]. Polli JW, Olson KL, Chism JP, John-Williams LS, Yeager RL, Woodard SM, Otto V, Castellino S, Demby VE. An unexpected synergist role of P-glycoprotein and breast cancer resistance protein on the central nervous system penetration of the tyrosine kinase inhibitor lapatinib (N-{3-chloro-4-[(3-fluorobenzyl)oxy]phenyl}-6-[5-({[2-(methylsulfonyl)ethy l]amino}methyl)-2-furyl]-4-quinazolinamine; GW572016). Drug Metab. Dispos. 2009; 37(2): 439–442. [PubMed: 19056914]

[170]. Guhlmann A, Krauss K, Oberdorfer F, Siegel T, Scheuber PH, Muller J, Csuk-Glanzer B, Ziegler S, Ostertag H, Keppler D. Noninvasive assessment of hepatobiliary and renal elimination of cysteinyl leukotrienes by positron emission tomography. Hepatology. 1995; 21(6):1568–1575. [PubMed: 7768501]

[171]. Hendrikse NH. Monitoring interactions at ATP-dependent drug efflux pumps. Curr. Pharm. Des. 2000; 6(16):1653–1668. [PubMed: 10974159]

[172]. Hendrikse NH, Kuipers F, Meijer C, Havinga R, Bijleveld CM, van der Graaf WT, Vaalburg W, de Vries EG. In vivo imaging of hepatobiliary transport function mediated by multidrug resistance associated protein and P-glycoprotein. Cancer Chemother. Pharmacol. 2004; 54(2): 131–138. [PubMed: 15118837]

[173]. Bhargava KK, Joseph B, Ananthanarayanan M, Balasubramaniyan N, Tronco GG, Palestro CJ, Gupta S. Adenosine triphosphate-binding cassette subfamily C member 2 is the major transporter of the hepatobiliary imaging agent (99m)Tc-mebrofenin. J. Nucl. Med. 2009; 50(7):1140–1146. [PubMed: 19525466]

[174]. Mavel S, Dikic B, Palakas S, Emond P, Greguric I, de Gracia AG, Mattner F, Garrigos M, Guilloteau D, Katsifis A. Synthesis and biological evaluation of a series of flavone derivatives as potential radioligands for imaging the multidrug resistance-associated protein 1 (ABCC1/MRP1). Bioorg. Med. Chem. 2006; 14(5):1599–1607. [PubMed: 16263302]

[175]. Takashima T, Nagata H, Nakae T, Cui Y, Wada Y, Kitamura S, Doi H, Suzuki M, Maeda K, Kusuhara H, Sugiyama Y, Watanabe Y. Positron emission tomography studies using (15R)-16-m-[^{11}C]tolyl-17,18,19,20-tetranorisocarbacyclin methyl ester for the evaluation of hepatobiliary transport. J. Pharmacol. Exp. Ther. 2010; 335(2):314–323. [PubMed: 20716623]

[176]. Okamura T, Kikuchi T, Okada M, Toramatsu C, Fukushi K, Takei M, Irie T. Noninvasive and quantitative assessment of the function of multidrug resistance-associated protein 1 in the living brain. J. Cereb. Blood Flow Metab. 2009; 29(3):504–511. [PubMed: 18985052]

[177]. Okamura T, Kikuchi T, Fukushi K, Irie T. Reactivity of 6-halopurine analogs with glutathione as a radiotracer for assessing function of multidrug resistance-associated protein 1. J. Med. Chem. 2009; 52(22):7284–7288. [PubMed: 19921956]

Pgp Substrates

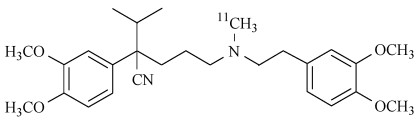

[^{11}C]Verapamil

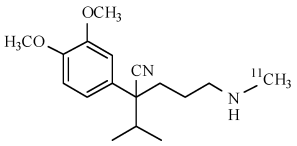

[^{11}C]D617

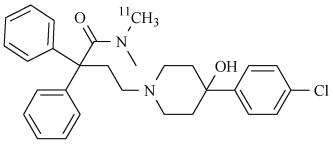

[^{11}C]Loperamide

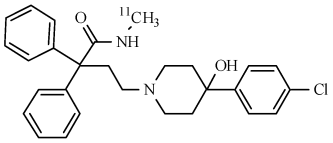

[^{11}C]-*N*-desmethyl-loperamide

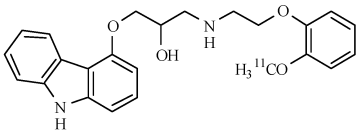

[^{11}C]Carvedilol

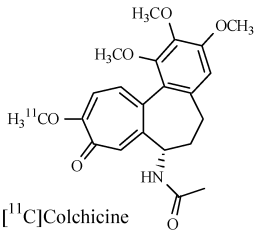

[^{11}C]Colchicine

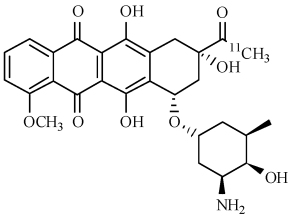

[^{11}C]Daunorubicin

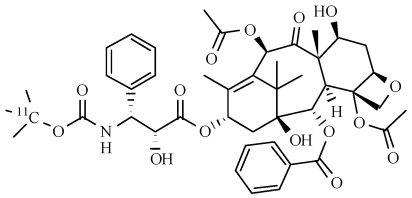

[^{11}C]Docetaxel

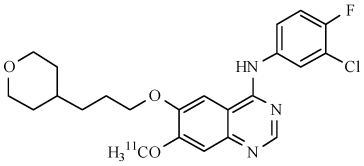

[^{11}C]Gefitinib

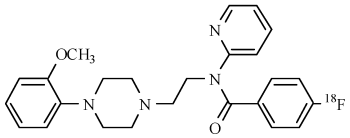

[^{18}F]MPPF

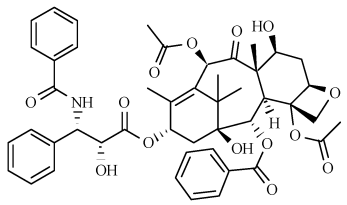

[^{11}C]Paclitaxel

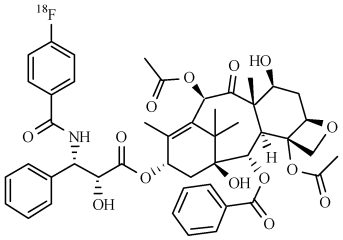

4-[^{18}F]Fluoropaclitaxel

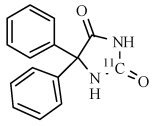

[^{11}C]Phenytoin

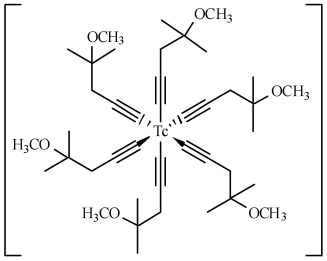

[^{99m}Tc]Sestamibi

Pgp Inhibitors

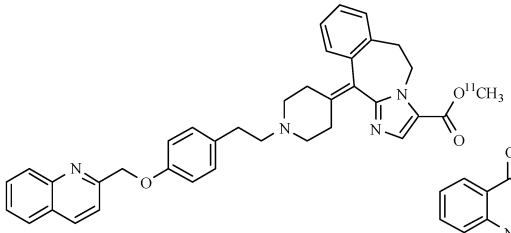

[^{11}C]Laniquidar

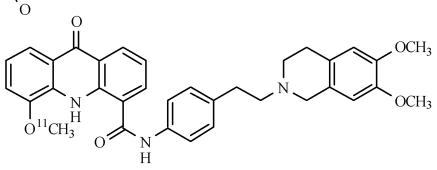

[^{11}C]Elacridar

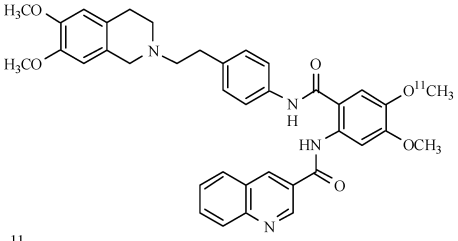

[^{11}C]Tariquidar

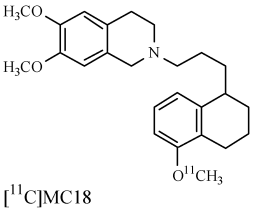

[^{11}C]MC18

Europe PMC Funders Author Manuscripts

Europe PMC Funders Author Manuscripts

BCRP Substrates and Inhibitors

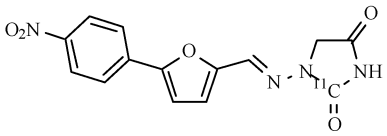

[^{11}C]Dantrolene

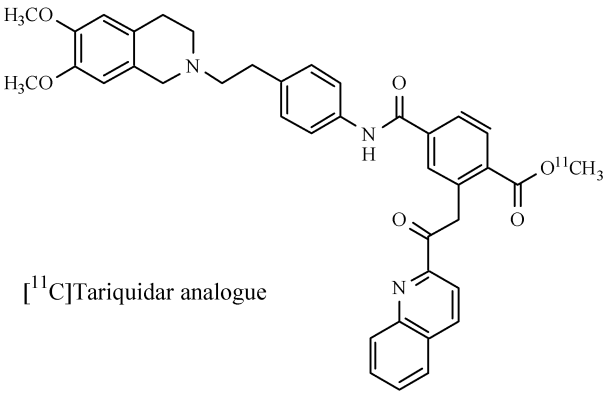

[^{11}C]Tariquidar analogue

MRP Substrates

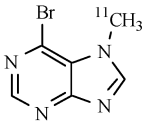

6-bromo-7-[^{11}C]methylpurine

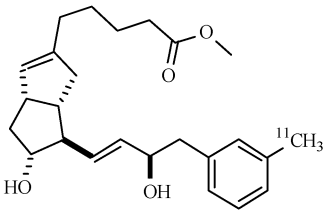

15R-[^{11}C]TIC-Me

Figure 1.
Chemical structures of ABC transporter PET and SPECT tracers discussed in this review article.